Final report for the grant of AOARD-06-4056

- **Title of Proposed Research :**

Vertical alignment of single-walled carbon nanotubes on nanostructure fabricated by atomic force microscope

- **Name of Principal Investigator :**

  Haiwon Lee

- **Affiliation of Researcher(s) :**

  Hanyang University

- **Address of Researcher(s) :**

  Department of Chemistry, Hanyang University, 17 Haengdang-dong, Seongdong-gu, Seoul 133-791, Korea
  Phone: +82-2-2220-0945
  FAX: +82-2-2296-0287

- Past AOARD or US government support

Report Documentation Page

1. REPORT DATE **30 MAR 2007**	2. REPORT TYPE	3. DATES COVERED

4. TITLE AND SUBTITLE	5a. CONTRACT NUMBER
Vertical alignment of single-walled carbon nanotubes on nanostructure fabricated by atomic force microscope	5b. GRANT NUMBER
	5c. PROGRAM ELEMENT NUMBER
6. AUTHOR(S) **Haiwon Lee**	5d. PROJECT NUMBER
	5e. TASK NUMBER
	5f. WORK UNIT NUMBER

7. PERFORMING ORGANIZATION NAME(S) AND ADDRESS(ES) **Hanyang University,Haengdang-dong, Seongdong-gu,Seoul 133-791,Korea (South),KE,133791**	8. PERFORMING ORGANIZATION REPORT NUMBER **AOARD-064056**

9. SPONSORING/MONITORING AGENCY NAME(S) AND ADDRESS(ES)	10. SPONSOR/MONITOR'S ACRONYM(S)
	11. SPONSOR/MONITOR'S REPORT NUMBER(S)

12. DISTRIBUTION/AVAILABILITY STATEMENT
Approved for public release; distribution unlimited.

13. SUPPLEMENTARY NOTES

14. ABSTRACT

This project focused on the behavior of single-wall carbon nanotubes (SWCNTs) in the electrophoresis cells and aligned growth of SWCNTs by thermal chemical vapor deposition on selectively deposited metallic nanoparticles. Field emission characteristics of vertically aligned SWCNTs films were also studied.

15. SUBJECT TERMS

16. SECURITY CLASSIFICATION OF:			17. LIMITATION OF ABSTRACT	18. NUMBER OF PAGES	19a. NAME OF RESPONSIBLE PERSON
a. REPORT **unclassified**	b. ABSTRACT **unclassified**	c. THIS PAGE **unclassified**		**22**	

Abstract

Our work has been concentrated on both a vertical alignment of single-walled carbon nanotubes (SWCNTs) using electrophoretic deposition and an aligned growth of SWCNTs on selectively deposited metal nanoparticles on modified substrate using thermal chemical vapor deposition (CVD). In the field of electrophoresis, the mechanism of SWCNTs behavior in the electrophoresis cells and vertical alignment of SWCNTs by ultra sonication treatment are investigated. And the effect of mixture voltage of AC and DC to the elimination of carbon impurity from the surface and inside of vertically aligned SWCNTs films during the electrophoretic deposition process was investigated. In the field of synthesis of carbon nanotubes (CNTs), the selective attachment of catalytic metal nanoparticles on chemically modified Si substrate was performed. The vertically aligned SWCNTs are successfully synthesized on chemically modified MgO/Si substrate using thermal CVD. The effect of NH_3 pretreatment to the synthesis of SWCNTs was also investigated. Various analytical methods such as AFM, SEM, and Raman enabled the characterization of the CNTs.

Introduction

CNTs are tubular carbon molecules with properties that make them potentially useful in extremely small-scale applications. They exhibit unusual strength and unique electrical properties. Accordingly, the number of both specialized and large-scale applications is growing constantly, including their use as conductive and high-strength composites, energy storage and energy conversion devices, sensors, field emission displays and radiation sources, hydrogen storage media, nanometer-sized semiconductor devices, probes, interconnects, etc.

To apply such SWCNTs to various technologies, well-aligned carbon nanotubes are desirable. To date, there have been a number of efforts for aligning carbon nanotubes with direct growth methods like CVD method. And, various methods for aligning chemically functionalized CNTs, such as self-assembly methods, hydrophilic/hydrophobic interactions and electrochemistry, have also been introduced because of their simplicity at ambient temperature and their applicability to relatively large areas. Recently, a direct current (DC) electrodeposition method has been applied to forming CNT films efficiently on substrates. The CNT films with high density produced by an electrodeposition, however, are randomly aligned and also pressured by strong electric field, resulting in almost flat CNT films accumulated with high randomness of orientation which limits their applications. Therefore, it is very important to demonstrate the chemical functionalization of CNTs, their attachment with controllable processes, and vertical alignments of CNTs.

On the other hand, some integrated nanoelectronic devices consist of semiconducting SWCNTs by removing conducting SWCNTs from the as-grown SWCNTs were reported. But, the selective synthesis of conducting or semiconducting SWCNTs has not been reported yet. The electrical property of SWCNTs is primarily dependent on their diameter and chirality. Furthermore the diameter of SWCNTs largely depends on the size of the catalytic metal nanoparticles, from which it is grown in a CVD process. Thus, to achieve uniform electrical properties for SWCNTs,

it is critical to have a narrow size distribution of the catalyst nanoparticles. The selective deposition of catalytic metal nanoparticles is also important to the integration of SWCNTs into nanoelectronic devices.

Approaches and results

1. The mechanism of SWCNTs behavior in the electrophoresis cells and vertical alignment.

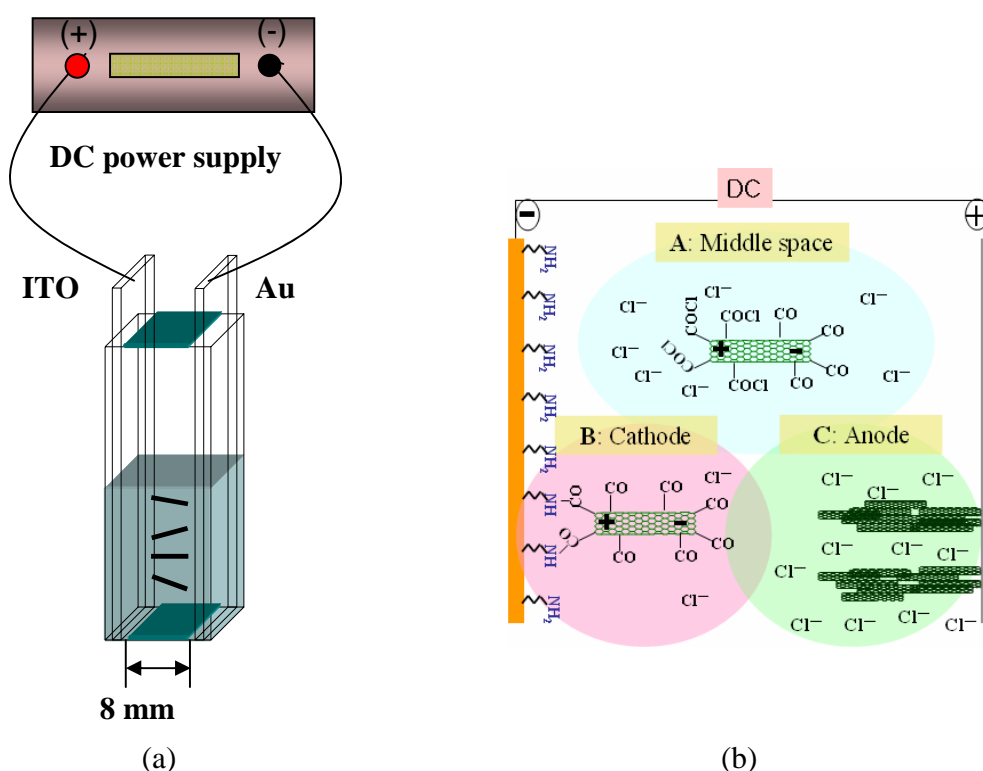(a)   (b)

Figure 1. Schematic view of (a) electrophoretic method and (b) the electrodeposition of COCl-SWCNTs in dimethyl formamide.

Figure 1(a) shows a simple schematic of a setup for electrodeposition. And Figure 1(b) suggests the electrodeposition process of SWCNTs-COCl in dimethyl formamide. When an electric field was applied to the SWCNT suspension, the SWCNT aggregates were produced immediately in the suspension. The SWCNTs-COCl, however, were well dispersed in dimethyl formamide (DMF) before applying an electric field. Since the stability in dispersion usually decreases with increasing ionic concentration, it is suggested that chloride ions are produced by dissociating from acid chloride groups on SWCNTs under the influence of DC field. In the middle space between two electrodes, the polarized SWCNTs under an electric field are stabilized in charge due to the compensation of chloride ions as shown in Figure 1(b) (A: middle space). The

SWCNTs near both electrodes migrated with a high speed toward the electrodes, caused by a strong charge interaction. On the cathode terminated with amine groups, a uniform SWCNT film was formed with a covalent bond as shown in Figure 1(b) (B: cathode). After prolonged deposition time, the coagulated SWCNTs were difficult to be deposited on the electrode because of its irregular shape. The dissociated chloride ions, Cl^-, migrate toward the positive electrode. The increase in the concentration of chloride ions near the anode resulted in the assembly of SWCNTs in a bundle as shown in Figure 1(b) (C: anode).
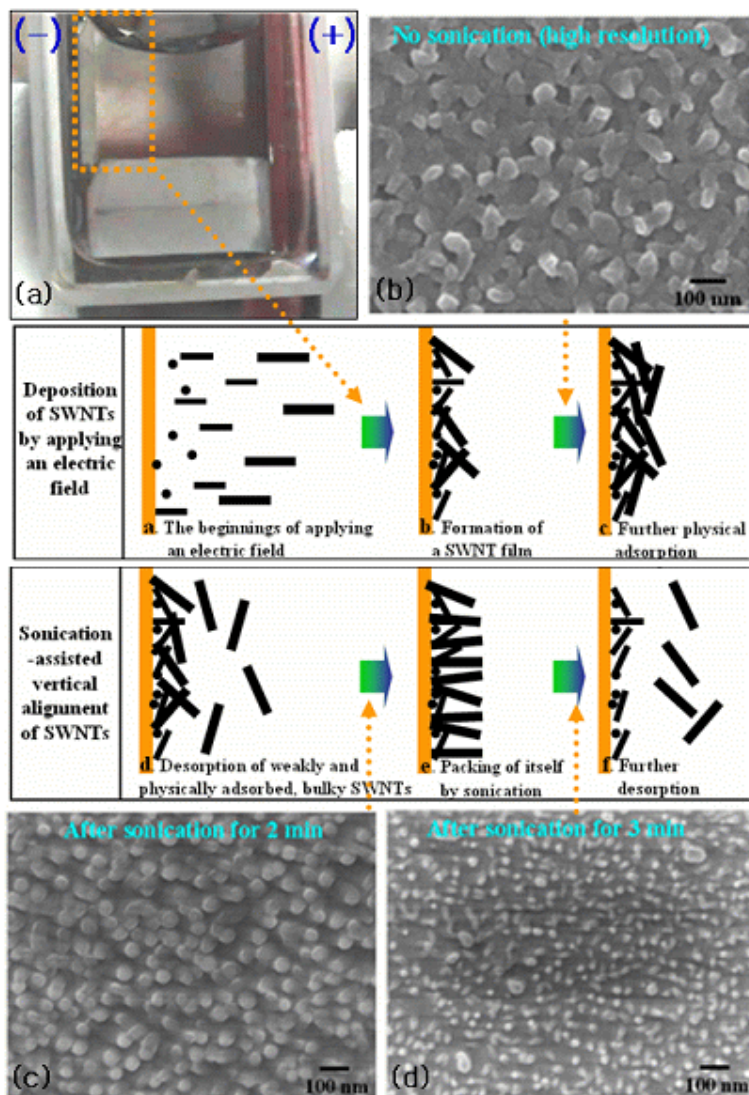

Figure 2. Schematic illustration of the formation of SWCNT film in a dc field and the perpendicular alignment of SWCNT bundles under the influence of sonication. (a) Actual cells containing a SWCNT suspension after applying an electric field between two electrodes separated by a 0.8cm gap. (b) SEM image of as-prepared SWCNT film formed on a gold electrode by applying an electric field at 150 V for 10 min. SEM images of the SWCNT film which remained on an gold electrode after ultrasonication for 2 min (c) and 3 min (d), respectively.

Figure 2 suggests the mechanism of the electrodeposition of SWCNT bundles and their perpendicular alignment by the assistance of sonication. Process a, SWCNTs are aligned parallel to an electric field in suspension and are deposited perpendicular to an electrodes under an applied electric field. Process b, SWCNT film is formed with a compressed form of SWCNT bundles in a few minutes. Process c, more SWCNTs are physically adsorbed and densely packed by a strong electric field for a prolonged adsorption time. Process d, weakly and physically adsorbed SWCNT bundles are detached at the beginning of sonication. Process e, SWCNT bundles are reassembled by self-packing under the influence of ultrasonic wave. Process f, further desorption is caused by prolonged sonication. We suggest here that densely deposited and compressed SWCNT bundles, which adhere via hydrophobic interactions, are annealed and aligned by ultrasonication. With increasing ultrasonication time, smaller SWCNTs with narrower diameter distributions appeared on the electrode due to desorption of bulky SWCNTs, as shown in Figures 2(c) and (d). Furthermore, we found that the SWCNT bundles were well distributed with uniform space between them and were mostly aligned normal to the surface after 3 min ultrasonication as shown in Figure 3. This method for aligning SWCNTs normal to the surface is comparable to CVD method or screen printing methods by which SWCNT films have been fabricated predominantly to date.
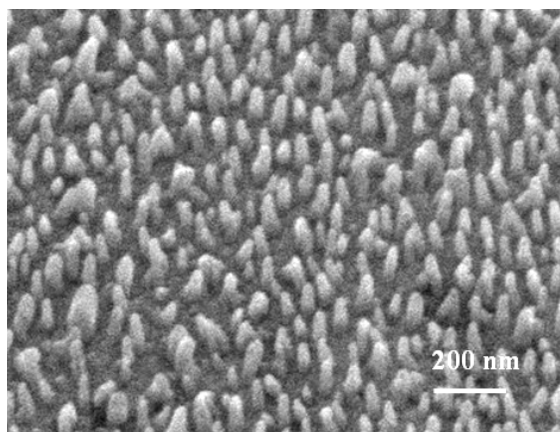

Figure 3. Tilted SEM image of vertically aligned SWCNT films formed on a gold substrate after ultrasonication for 3 min.

2. Electrophoretic deposition of vertically aligned SWCNTs with a mixture of AC and DC voltage.

2-1. Particle removal by effect of AC voltage

The electrodeposition by AC voltage was accomplished to compare with the effect of DC voltage. The gap distance between two electrodes were become narrow by 0.1 mm. AC voltage of 10 V_{p-p} was applied with a frequency of 10 kHz, 100 kHz, 1 MHz and 10 MHz, respectively. As the frequency added on electrode was increased, particles or impurities were removed and only SWCNTs-COCl was attached, as shown in Figure 4, because the polarity of electric field is periodically shifted in AC voltage. Contrary to this, SWCNT films were formed by electric field of DC voltage in gap having 100um. Gold substrates were covered with thick SWCNT films as shown in figure 5.
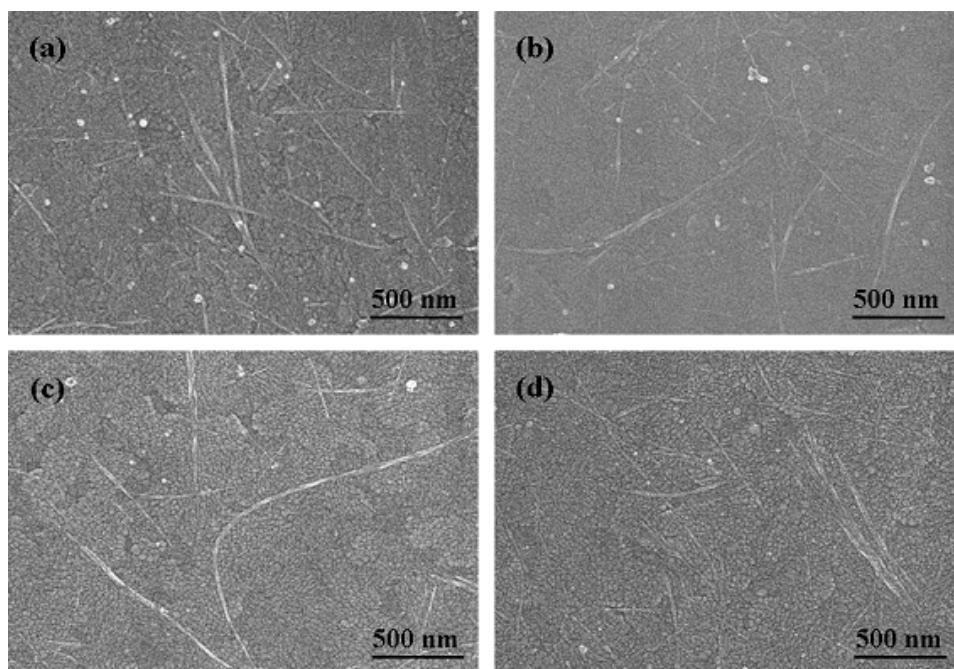
Figure 4. SEM images of the attached SWCNTs in condition of AC electric field. Under the voltage of 10 V$_{p-p}$, frequency was added by (a) 10 kHz, (b) 100kH, (c) 1MHz and (d) 10 MHz.
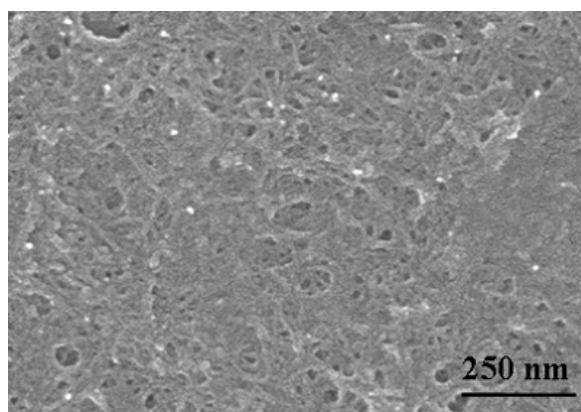

Figure 5. SEM image of the SWCNTs film formed by electrodeposition of DC voltage in gap having 100 um for 10 min.

2-2. Adsorption of SWCNTs by the combined electric field of DC and AC voltage

A combined electric field of DC voltage of 10 ~ 40V and AC voltage of 10Vp-p with a frequency of 1 MHz was used to adsorb SWCNTs on substrate. Figure 6 shows SEM images of SWCNTs attached on a gold electrode by applying the mixture of DC and AC voltage. When DC voltage of 10V was applied, few SWCNTs are attached. The amount of attaching SWCNTs has

increased with the DC voltage. When the DC voltage of 40 V was applied, SWCNT bundles were attached on gold electrode separately with a high density as shown in Figure 7. They were anchored on gold substrate having cylindrical shape without carbon particles and damaged SWCNTs.
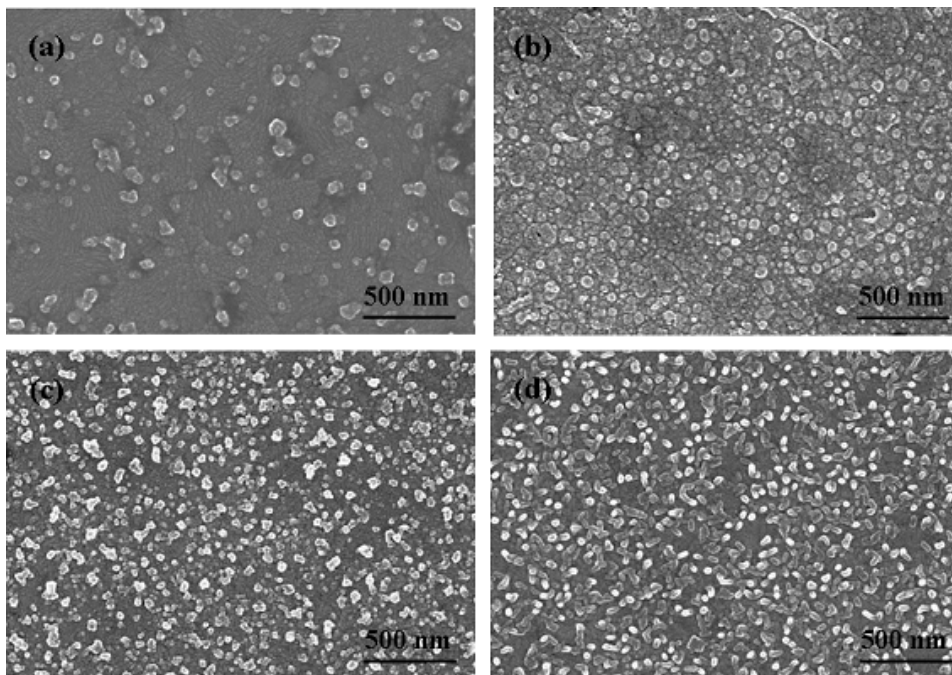

Figure 6. SEM images of SWCNTs anchored on gold substrate applying combined electric field of DC and AC voltage. When DC voltage of (a) 10 V, (b) 20 V, (c) 30V and (d) 40V was applied with the AC voltage of 10V$_{p-p}$, each case showed a different appearance.
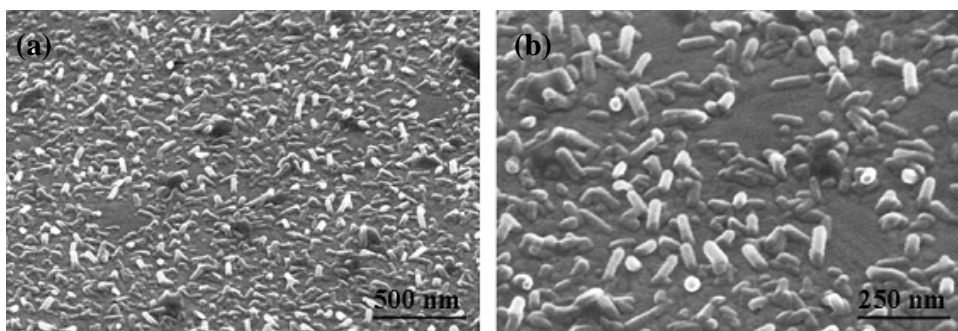

Figure 7. Tilted SEM images of SWCNTs applying DC voltage of 40 V and AC voltage of 10 V. (b) is the magnified image of (a).

Figure 8 is the Raman spectrum of vertically aligned SWCNTs deposited on gold substrates using electrophoresis with combined electric field of DC and AC voltage. It shows typical Raman properties of SWCNT including strong G band (1587 cm^{-1}), weak D band (1340 cm^{-1}) and clear RBM band (186 cm^{-1}). According to the Raman spectrum, the crystallinity of SWCNTs electrodeposited on the gold substrate was known to be preserved even after electrodeposition at a high speed of migration.
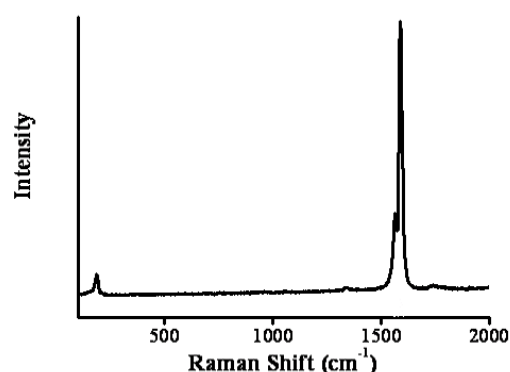
Figure 8. Raman spectrum of vertically aligned SWCNTs electrodeposited on gold substrates using combined electric field of DC and AC voltage.

3. Aligned growth of SWCNTs using thermal CVD on selectively deposited metal nanoparticles.
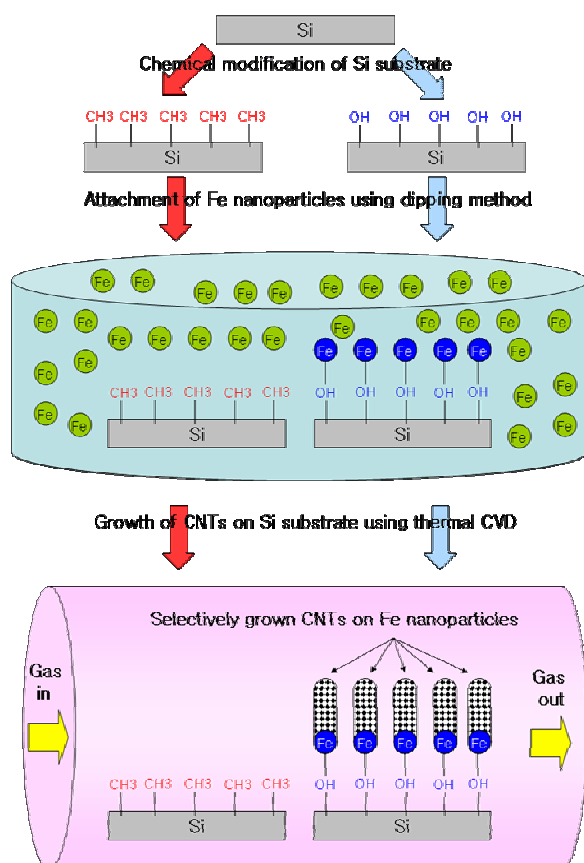

Figure 9. Scheme of process for the synthesis of CNTs on selectively adsorbed Fe catalytic metal nanoparticles on chemically modified Si substrate using dipping method.

3-1. Growth of CNTs on the selectively deposited catalytic metal nanoparticles on chemically modified Si substrate.

The vertically aligned CNTs were synthesized on catalytic metal nanoparticles which were adsorbed on chemically modified Si substrate using dipping method. Figure 9 is the scheme of process for the synthesis of CNTs on selectively adsorbed Fe catalytic metal nanoparticles on chemically modified Si substrate using dipping method. The UV irradiated ozone was introduced to the surface of bear Si substrate to making a hydrophilic surface. The hydrophobic surface of Si substrate was prepared by dipping the hydrophilic Si substrate into the octadecyltrichlorosilane (OTS) solution (3 mM OTS in Toluene) for 1 hour, and fully rinsed with pure toluene. The Fe catalytic metal nanoparticles were formed on modified Si substrate by dipping a Si substrate into the Fe solution (0.05 M of $FeCl_3$ in 100 mL of ethanol) for 5 min and rinsing with pure ethanol. Vertically aligned CNTs were synthesized by catalytic decomposition of C_2H_2 at 800 ℃ for 10 min using thermal CVD. Figure 10 shows optical images and AFM

images of Fe catalytic metal nanoparticles adsorbed on the hydrophilic and hydrophobic Si substrate, respectively. It clearly shows that the Fe catalytic metal nanoparticles were adsorbed on all over the surface of hydrophilic Si substrate with high density, but there are few Fe catalytic metal nanoparticles on the hydrophobic Si substrate.
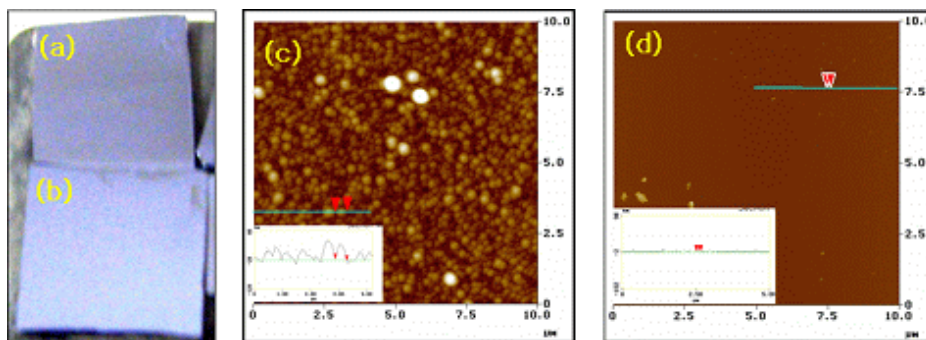

Figure 10. Optical images ((a), (b)) and AFM images ((c), (d)) of Fe catalytic metal nanoparticles adsorbed on hydrophilic ((a), (c)) and hydrophobic ((b), (d)) Si substrate, respectively. The size of Si substrate is about 1 x 1 cm^2.

Figure 11 shows optical images and SEM images of CNTs grown on Fe catalytic metal nanoparticles adsorbed on the modified Si substrate using thermal CVD. It clearly shows that the vertically aligned CNTs were grown on hydrophilic Si substrate, but few CNTs were grown on hydrophobic Si substrate. The existence of a few of CNTs shown in figure 11(d) is originated from the unexpected adsorption of Fe catalytic metal nanoparticles on defect site of OTS SAM on Si substrate. Our results are promising for the selective growth of vertically aligned CNTs on a large-area Si substrate using a simple catalyst deposition process.
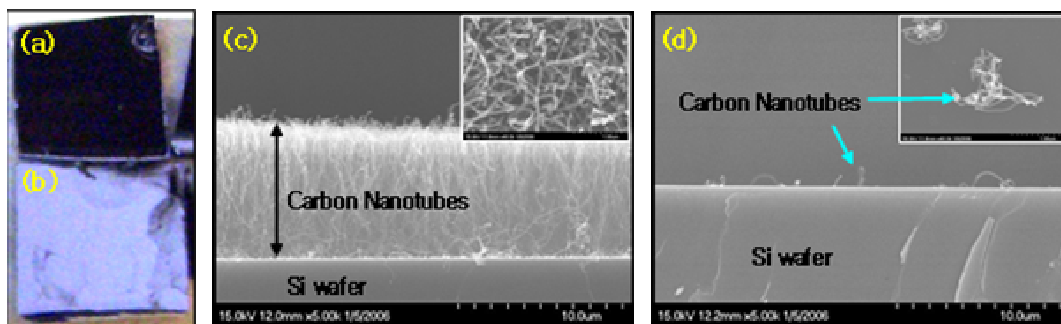
Figure 11. Optical images ((a), (b)) and AFM images ((c), (d)) of CNTs grown on hydrophilic ((a), (c)) and hydrophobic ((b), (d)) Si substrate, respectively. The size of Si substrate is about 1 x 1 cm^2. SEM images of the inset of (c) and (d) are enlarged top view images of each sample.

3-2. Growth of vertically aligned SWCNTs on Si substrate using thermal CVD.
The Fe-Mo catalytic metal nanoparticles were adsorbed on MgO coated Si substrate by dipping a hydrophilic MgO/Si substrate into the Fe-Mo solution (Fe 0.01M and Mo 0.01M in Ethanol 50 ml). The Fe-Mo/MgO/Si substrate was pre-treated with NH$_3$ at 800 ℃ for 10 min. The vertically aligned SWCNTs were synthesized on Fe-Mo/MgO/Si substrate by catalytic decomposition of

C$_2$H$_2$ using thermal CVD. Figure 12(a) is the SEM images of vertically aligned SWCNTs films on Fe-Mo/MgO/Si substrate. The thickness of SWCNTs film is 5 um. The inset image of Figure 12(a) shows that the SWCNTs have a noodle shape without carbon impurities. Raman spectra of vertically aligned SWCNTs clearly showed that the as synthesized CNTs are SWCNTs and have various diameters as shown in Figure 12(b).
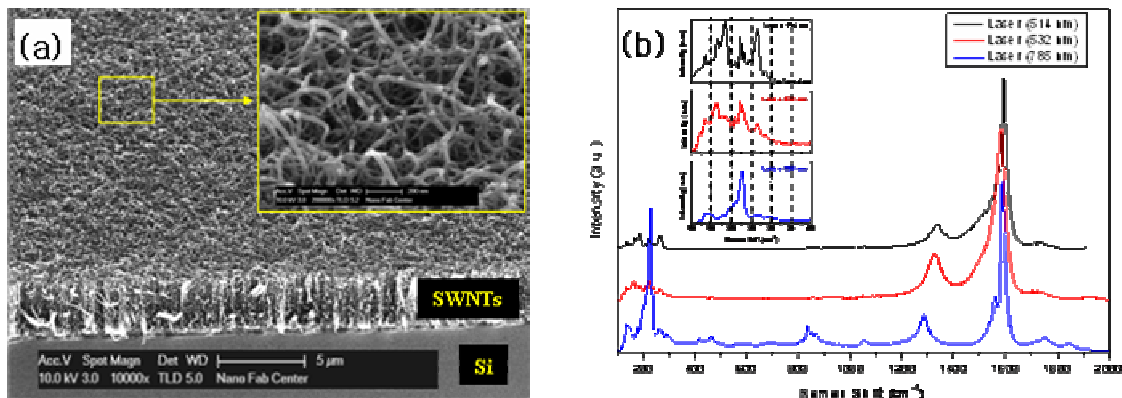
Figure 12. SEM images (a) and Raman spectra (b) of vertically aligned SWCNTs on Fe-Mo/MgO/Si substrate using thermal CVD.
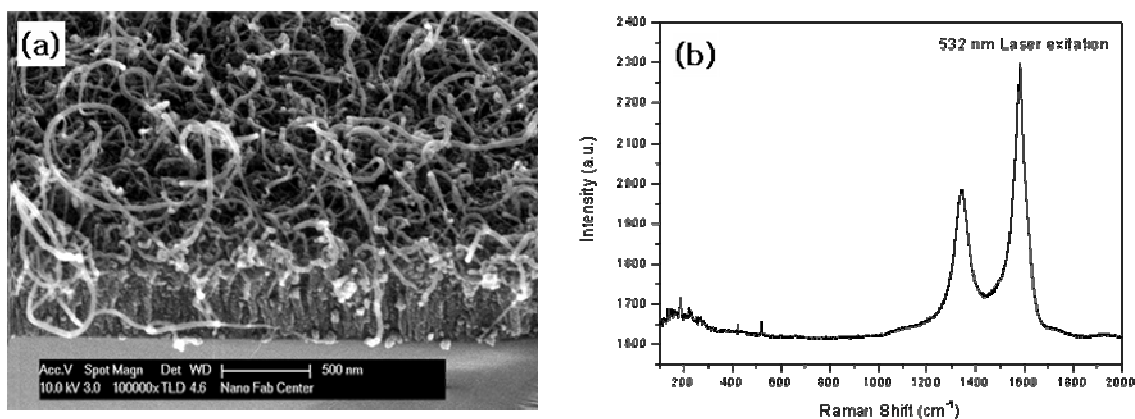
Figure 13. SEM image (a) and Raman spectrum (b) of CNTs grown on Fe-Mo/MgO/Si substrate without NH$_3$ pretreatment using thermal CVD.

It was found that the NH$_3$ pretreatment affects the growth and vertical alignment of SWCNTs on Fe-Mo/MgO/Si substrate using thermal CVD. Figure 13 shows SEM image and Raman spectrum of CNTs grown on Fe-Mo/MgO/Si substrate without NH$_3$ pretreatment using thermal CVD. CNTs were not aligned on MgO/Si substrate with a low density. The Raman spectrum shows a strong D peak and some week peaks at RBM frequency. SEM and Raman results indicate the existence of large amount of carbon impurities or multi-walled carbon nanotubes (MWCNTs) and few of SWCNTs in the as-grown CNTs

4. The effect of NH₃ pretreatment to the diameter and the vertical alignment of SWCNTs.

It was reported that the atomic hydrogen reduces the metal oxides to the pure metals resulted in increasing efficiency of metal catalyst for the synthesis of CNTs. And, the atomic hydrogen is easily obtained by thermal decomposition of NH_3 at the low temperature. Thus, the NH_3 pretreatment on the metals catalyst has been used for the synthesis of MWCNTs on Si substrate using thermal CVD. But, there is no report on the NH_3 pretreatment on catalytic metal nanoparticles for the synthesis of SWCNTs using thermal CVD. We investigated the effect of NH_3 pretreatment to the synthesis of SWCNTs. Figure 14 is the SEM images of SWCNTs grown on Fe-Mo/MgO/Si substrate using thermal CVD with different NH_3 pretreatment conditions at 800 ℃. It shows that the diameter and density of SWCNTs increase with the flowing rate of NH_3. Figure 14(d), (e), and (f) are show that the vertically aligned SWCNTs were grown on Fe-Mo/MgO/Si substrate by increasing the flowing rate of NH_3 at the NH_3 pretreatment process. It seems that the SWCNTs are vertically aligned due to the effect of studied hindrance between the SWCNTs.
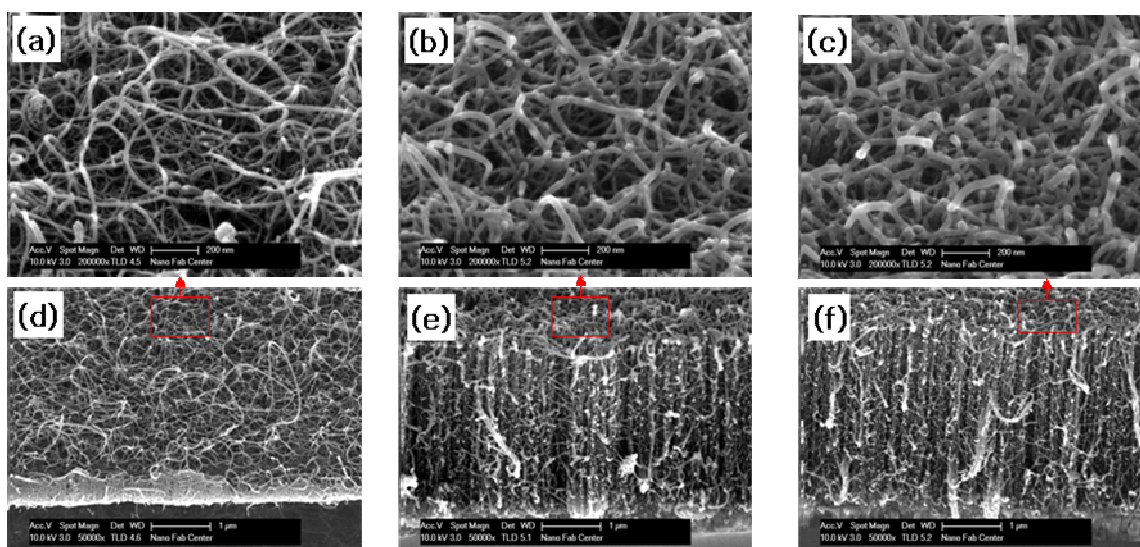

Figure 14. SEM images of SWCNTs grown on Fe-Mo/MgO/Si substrate using thermal CVD with different NH₃ pretreatment conditions at 800 ℃. The flowing rate of NH₃ is 50 sccm (a, d), 250 sccm (b, e), and 500 sccm (c, f), respectively.

Figure 15 shows the Raman spectra of as-synthesized SWCNTs depending on the NH_3 pretreatment conditions. They show the general Raman spectrum shape of SWCNTs which have strong G bands at 1582-1587 cm⁻¹ with high intensity, weak D bands at 1331 cm⁻¹ with low intensity and clear peaks in RBM area of 100–400 cm⁻¹. Figure 15(a) is enlarged spectra of the radial breathing mode (RBM) frequency areas of 100–400 cm⁻¹. The upper X axis of Figure 15(a) indicates the SWCNTs diameter calculated from the Raman frequency. For the calculation of SWCNTs diameter, the equation (ω_r (cm⁻¹) = 12.5 + 223.5/d (nm)) was used. In this equation, ω_r is the Raman frequency and d is the SWCNTs diameter. The Raman spectra of RBM frequency area clearly show that the amount of SWCNTs with small diameter decreases with increasing the flowing rate of NH_3.
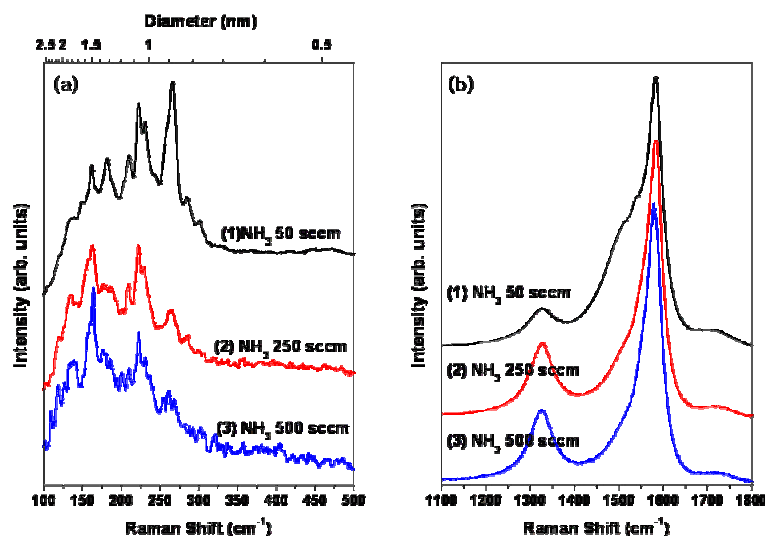
Figure 15. Raman spectra of SWCNTs depending on the NH_3 pretreatment conditions. The wave length of source laser is 532 nm. (a) Raman spectra of RBM frequency. (b) Raman spectra of G band and D band frequencies. Spectrum (1): NH_3 pretreatment 50 sccm 10 min, Spectrum (2): NH_3 pretreatment 250 sccm 10 min, Spectrum (3): NH_3 pretreatment 500 sccm 10 min.

Summary

The mechanisms of SWCNTs behavior in the electrophoresis cells and the vertical alignment of SWCNTs by assistance of ultra sonication were investigated. The electrodeposition by AC voltage was accomplished to compare with the effect of DC voltage. As the frequency of AC voltage was increased, carbon particles and other impurities were removed and only SWCNTs-COCl was attached on the gold electrode. When the combined electric field of DC and AC was applied, the clean and vertically aligned SWCNTs were deposited on a gold electrode with high density, which may contribute to applying SWCNTs as an electron emission sources in nanoelectronic devices. It was investigated that the catalytic metal nanoparticles are selectively deposited on a chemically-modified Si substrate by dipping method. As a result, our novel method is promising for the selective growth of vertically aligned CNTs on a large-area Si substrate using a simple catalyst deposition process. Based on this method, the vertically aligned SWCNTs were successfully synthesized on a Fe-Mo/MgO/Si substrate using thermal CVD. It was found that the SWCNTs are vertically aligned on substrate by introducing the NH_3 pretreatment process on catalytic metal nanoparticles. The diameter and the density of SWCNTs were controlled by adjusting the flowing rate of NH_3 at the NH_3 pretreatment process. Our experimental results offer possibility in the integration of SWCNTs into nanoelectronic devices.

Publications

[1] "Ramified fractal-patterns formed by droplet evaporation of a solution containing single-walled carbon nanotubes", Jianlong Zhang, Sung-Kyoung Kim, Xiudong Sun, Haiwon Lee, Colloids and Surfaces A: Physicochem. Eng. Aspects 292 (2007) 148-152.
[2] "Characteristics of Electrodeposited Single-Walled Carbon Nanotube Film", Sung-Kyoung Kim, Hee-Young Choi, Ha-Jin Lee, and Haiwon Lee, J. Nanosci. Nanotech. 6 (2006) 1-5.
[3] "Vertical Alignment of Single-Walled Carbon Nanotube Films Formed by Electrophoretic Deposition", Sung-Kyoung Kim, Haiwon Lee, Hirofumi Tanaka, Paul S. Weiss, Adv. Mater (In final revision)

Ramified fractal-patterns formed by droplet evaporation of a solution containing single-walled carbon nanotubes

Jianlong Zhang [a], Sung-Kyoung Kim [b], Xiudong Sun [a,**], Haiwon Lee [b,*]

[a] *Department of Physics, Harbin Institute of Technology, Harbin 150001, PR China*
[b] *Department of Chemistry, Hanyang University, Seoul 133-791, Republic of Korea*

Abstract

Single-walled carbon nanotubes (SWNTs) in aqueous and ethanol solutions can be self-assembled into ramified fractal-patterns, ring-patterns or fingering-patterns on silicon wafers over a large area under controlled evaporation conditions by the droplet evaporation method. The formation of these regular patterns can be attributed to the Marangoni effect and diffusion-limited aggregation (DLA) in the liquid film during droplet evaporation at different conditions. This simple method to assemble SWNTs will provide potential applications for advanced devices and sensors.
© 2006 Elsevier B.V. All rights reserved.

1. Introduction

The attention given to single-walled carbon nanotubes (SWNTs) has intensified recently because their unique chemical and physical properties make them a perfect candidate for a 1D material in nano-electronics [1,2]. Due to their potential applications, SWNTs could be incorporated into arrays or other special patterns. Using Langmuir-Blodgett and self-assembly methods, SWNTs are patterned selectively onto various substrates [3,4]. Zhou et al. assembled SWNTs into aligned films and regular patterns on glasses using a slow evaporation method [5]. In fact, the processing of nanoparticles into large rings or hexagonally compact networks with silver [6,7] and ferrite nanocrystals [8] has been reported. Via microcontact printing (μCP), it is possible to more precisely assemble polystyrene latex spheres into regular arrays [9]. Also the fractal patterns of particles have been obtained by methods such as fractal hole growth [10], electrodeposition [11], viscous fluid flowing [12] and microcontact printing [13]. However, similar results related to SWNTs have not yet been reported. In this study, a simple method using droplet evaporation to form fractal, ring- or fingering-patterns of the SWNTs on silicon wafers is introduced and discussed for the first time.

2. Experiment

Raw SWNTs with a purity of 97% were synthesized by the chemical vapor deposition (CVD) method, purified in a 5 mM HCl solution for an additional 3 h and were then etched into short SWNTs in a mixed acid solution of H_2SO_4 (98%):HNO_3 (70%) = 3:1 (v/v) for 7 h at 50 °C assisted by ultrasonication [14]. The collected short SWNTs were dispersed in DI water or ethanol by ultrasonication. The morphology of the short SWNTs was confirmed by SEM as shown in Fig. 1. The average length of the short SWNTs was estimated as 1 μm and the etched SWNTs were clean, which indicated that most of the impurities had been removed. Droplets of the SWNTs in ethanol and DI water solutions of different pH values were dropped onto the silicon wafers of 1 cm × 1 cm and processed and rinsed by HPLC grade ethanol and DI water, a Piranha treatment or coated by an octadecyltrichlorosilane (OTS) self-assembled monolayer. Then the SWNT droplet was evaporated under controlled ambient conditions (room temperature and humidity) and then the dried wafers were examined by optical microscopy.

* Corresponding author. Tel.: +82 2 2220 0945; fax: +82 2 2296 0287.
** Co-Corresponding author. Tel.: +82 451 8641/4129;
fax: +82 451 8641/4129.
E-mail addresses: xdsun@hit.edu.cn (X. Sun),
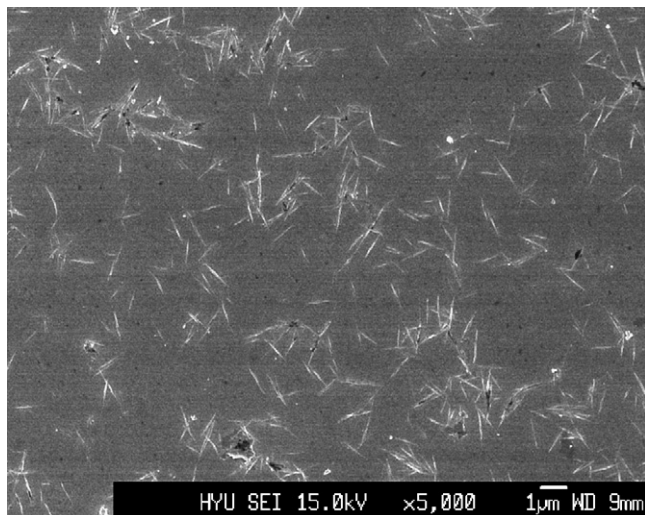haiwon@hanyang.ac.kr (H. Lee).

Fig. 1. SEM image of the short SWNTs on a silicon wafer after being etched in a mixed acid.

3. Results and discussion

If the evaporation conditions are not controlled the SWNTs usually exist as random aggregations on silicon surfaces after aqueous droplets of the SWNTs are air-dried. However, with controlled evaporation conditions, the SWNTs formed ramified fractal-patterns with different shapes over a large area. Fig. 2(a) and (b) show high-resolution optical photographs of such pat-

terns fabricated at an evaporation temperature of 23 °C, a relative humidity of 60%, a concentration of 0.05 mg/ml and a pH of 6. Pattern growth always began inward from the droplet boundary. The growth direction was either vertical or parallel to the boundary depending on the direction of solution flow during evaporation. The SEM image shown in Fig. 1 and the energy dispersive X-ray (EDX) spectrum (see Fig. S1) show that there were no impurities such as metal catalysts in the SWNTs solution and that the formed ramified fractal-patterns consisted only of SWNTs. However, if the contact angle of the silicon wafers and water was below 5° as etched by the Piranha treatment, the SWNT droplet would spread onto the whole surface and no ramified fractal-patterns were found after drying. Similarly, if the SWNT solution was dropped onto the silicon wafers modified with an OTS monolayer [15], the SWNT droplet had a water contact angle of 103.49° and the SWNTs in the droplet would aggregate randomly after evaporation. Thus, the water contact angle was an important parameter for forming ramified SWNT fractal-patterns and required an appropriate hydrophobic nature of the silicon wafer. In light of this, a clean silicon wafer rinsed by ethanol or water was good for forming ramified fractal-patterns of the SWNTs. When ethanol was used as a solvent, ramified fractal-patterns of SWNTs were formed on the clean silicon wafer (see Fig. S2).

A possible mechanism regarding how SWNTs form ramified fractal-patterns is attributed to the diffusion-limited aggregation (DLA) model [16–18]. Ramified fractal-patterns of SWNTs can be formed as follows: a seed SWNT bundle is fixed at a starting
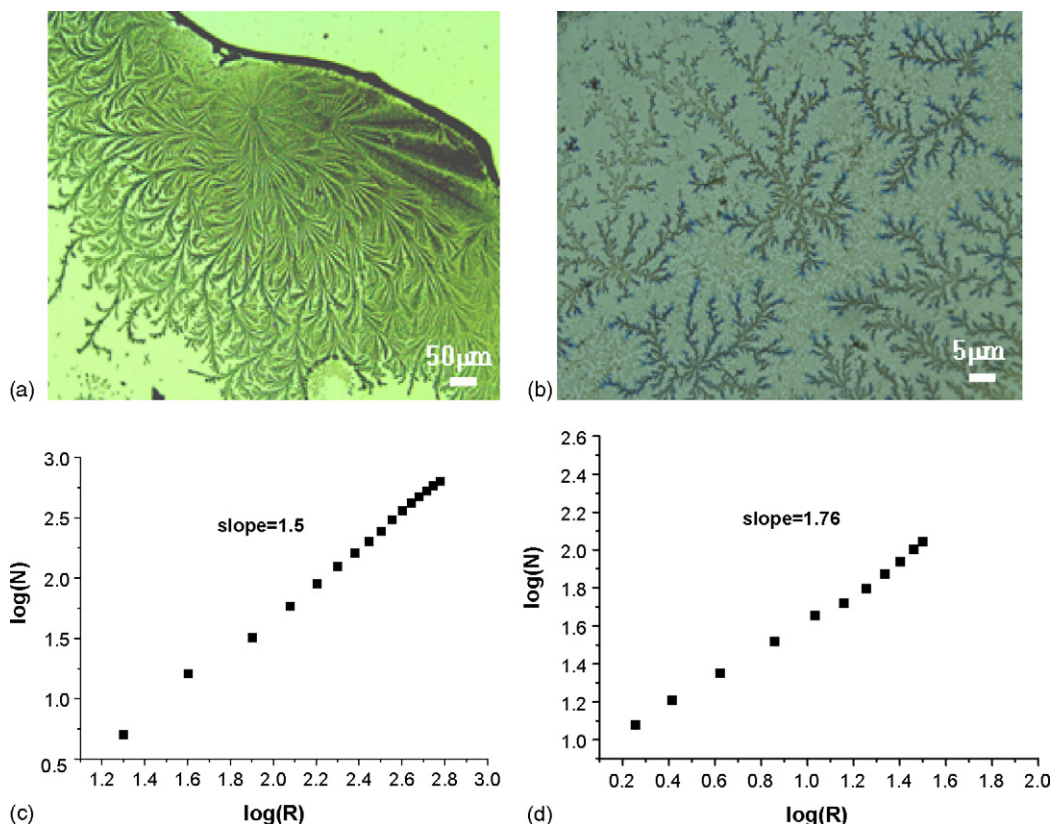
Fig. 2. Optical micrographs (a, b) of the ramified patterns of the SWNTs on the silicon surface and log–log plots of N and R (c, d) according to the figures of (a) and (b). R is the radius of the centric circles in pixels and N the number of pixels in the circle that are covered by SWNT fractals.
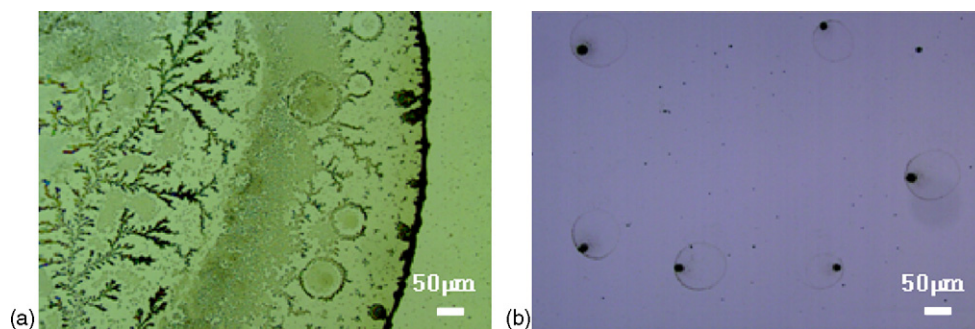
Fig. 3. Optical micrographs of the ring-patterns on the silicon wafers when water (a) and ethanol (b) was used as the solvent to immerse the SWNTs.

Fig. 4. Optical micrographs of the fingering patterns of the SWNTs on silicon wafers (a–d) at a temperature of 14 °C and relative humidity of 75%, in which the droplet volume was 5 μl, 10 μl, 20 μl, and 25 μl for a–d, respectively; (e) the dependence of the fingering-pattern length on the droplet volume.

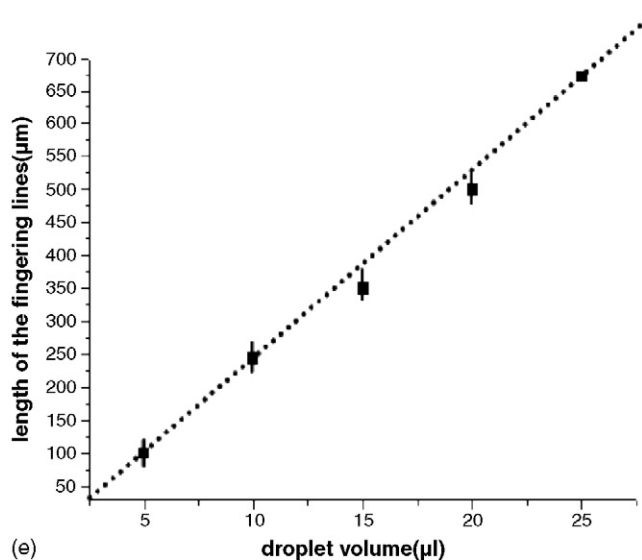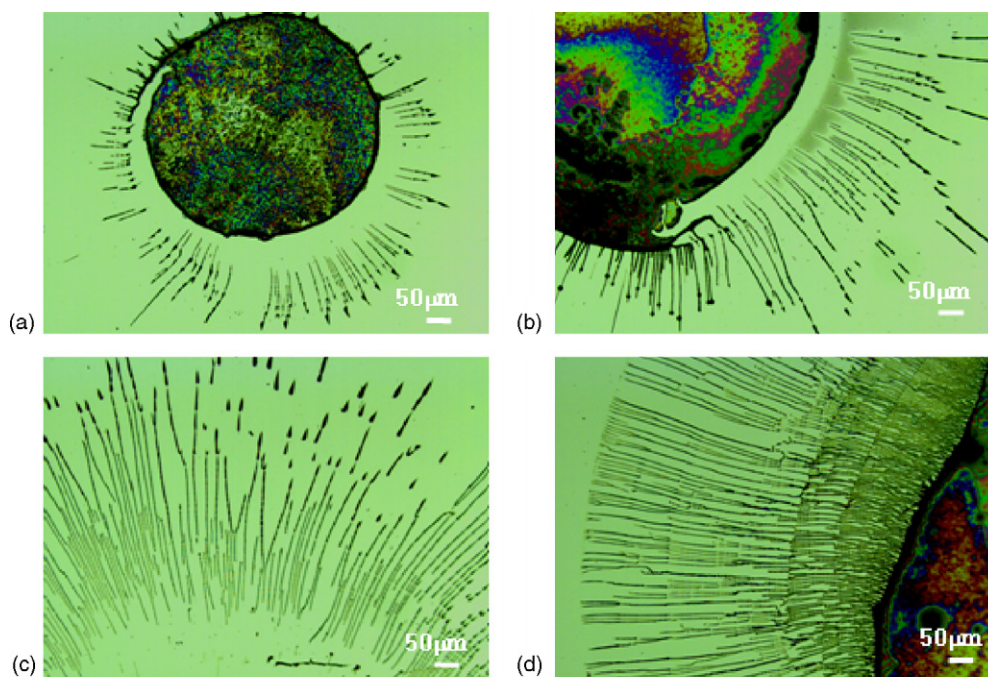point, and then a random walking SWNT bundle is launched through lateral capillary forces [19] until it touches the seed and stops. Then, another walking SWNT bundle is launched and diffuses until it touches one of the first two, and so on. Thus, many SWNT bundles are tethered from the seed SWNT bundle to assemble into ramified fractal-patterns. Based on this model, Fig. 2(c) and (d) show the density fractal-dimensions of the ramified fractal-patterns depicted in Fig. 2(a) and (b). The slopes of such curves were roughly estimated as 1.5 and 1.76, respectively, using a previously described method [20]. These values are very close to the reported typical values of the ramified fractal-patterns formed via the DLA model [10,21,22]. Thus, it is reasonable to attribute the formation of the ramified fractal-patterns of the SWNTs to the DLA model.

When water was used as a solvent to immerse the SWNTs, ring-patterns could also be found in the ramified fractal-patterns of the SWNTs as shown in Fig. 3(a). Such ring-patterns are often formed due to the Marangoni effect when a volatile solvent is used as the evaporation solvent [23]. The formation of such ring-patterns appeared to be related to a short evaporation time. A short evaporation time can increase the Marangoni number and then induce a high degree of instability in the liquid film. Our experiments confirmed these results. Fig. 3(b) shows an optical micrograph of many ring and dot patterns in a micrometer scale formed on the silicon wafers when ethanol was used as the dropping solvent. It is obvious that there are more ring-patterns in Fig. 3(b) than in Fig. 3(a). This suggests that the short evaporation time (the evaporation time was 15 s for ethanol at 25 °C and a relative humidity of 65%) could induce strong instabilities in the liquid film, which in turn induced the formation of a mixture of ring and dot patterns. This process can be depicted as follows: in liquid evaporation, when a liquid droplet is almost completely evaporated and only a very thin film remains, the thin film would also experience the Marangoni effect due to the local instabilities that are facilitated by using a volatile solvent, and then some holes are formed. The opening holes push the SWNTs outward along their advancing rims. When the friction between the SWNTs and the substrate is high enough to prevent the diffusion of the SWNTs, the SWNT aggregations can be pinned near the contact line of the holes to form ring-patterns.

Factors such as the evaporation temperature, humidity, the pH of the SWNT solution and the concentration of the SWNTs affect the formation of the SWNT fractal patterns. When the temperature was controlled between 10 and 35 °C, the humidity was maintained between 45 and 75%, the pH of the SWNTs solution was adjusted near 6 and the concentration of SWNTs was fixed near 0.05 mg/ml, ramified fractal-patterns were formed on the clean silicon wafers. When the relative humidity was higher than 75%, fingering-patterns instead of the ramified fractal-patterns were formed near the boundary lines of the SWNTs aggregation. Fig. 4 shows that such patterns developed when evaporated at a temperature of 14 °C, a relative humidity of 75%, a SWNT concentration of 0.05 mg/ml and a pH of 6. This phenomenon is similar to the results reported in a previous study [23]. The length of the periodic patterns could be several hundreds of micrometers linearly, depending on the volume of the initial SWNTs droplet, as shown in Fig. 4e. The ends of the fingering-patterns
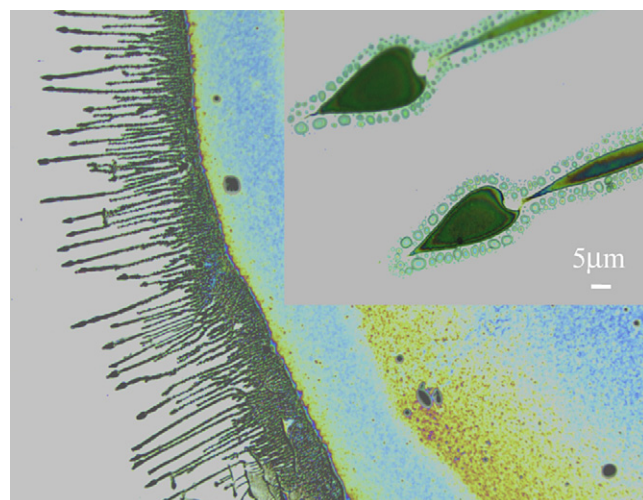

Fig. 5. Optical micrograph of the fingering-patterns of the SWNTs on a silicon wafer.

were flat or arrow-like. Thereby the temperature and humidity determined the evaporation speed and the wetting conditions at the interface of the droplet and the silicon surface, which resulted in the formation of different patterns. Fast evaporation under circumstances of low humidity can induce a well-ordered aggregation of the SWNTs through long-range attractive interactions and lateral capillary forces while slow evaporation under conditions of high humidity induced the fingering-pattern formation in the wet water film. Fig. 5 shows a higher resolution photograph of the fingering-patterns fabricated at an evaporation temperature of 14 °C, a relative humidity of 65%, an SWNT concentration of 0.05 mg/ml and a pH value of 2. There were many periodic dots surrounding the fingering lines with arrow-like shapes, which were believed to be related to the interactions of the silicon surface and the residual acids in the droplet after the SWNTs were collected from the etching acids. The arrow-like shape of the fingering-pattern and the periodic dots around it may be a result of the dewetting effect [24]. During the evaporation of the liquid film, the wetting frontline was unstable and caused fingering. The liquid flow proceeded along these fingering-patterns and the SWNTs in the flow path were deposited due to this instability. In order to obtain ramified fractal-patterns, the residual acid should be removed to keep the pH value of the SWNTs solution near 6.

In all, it was possible for both the Marangoni effect and DLA to occur during evaporation at different evaporation conditions. Once local instabilities during evaporation occurred, the SWNTs formed ramified fractal-, fingering- or ring-patterns according to the different evaporation conditions.

4. Conclusion

In conclusion, we demonstrated for the first time the ability to control the aggregation of SWNTs by the droplet evaporation method in air. The SWNTs formed three different shapes including ramified fractal-patterns, ring- and fingering-patterns on silicon wafers due to adjustments of concentration, purity and pH of the SWNT solution, temperature, air humidity, hydropho-

bic properties of the silicon wafers surfaces and the volume of the SWNTs droplet. The formation of ramified fractal-patterns can be explained by DLA while the ring- and fingering-patterns can be explained by the Marangoni effect in thin liquid films during evaporation. This simple method provides guidelines for assembling SWNTs into useful devices and sensors.

Acknowledgements

Appendix A. Supplementary data

Supplementary data associated with this article can be found, in the online version, at doi:10.1016/j.colsurfa.2006.06.022.

References

[1] S. Iijima, Nature 354 (1994) 56.
[2] P.M. Ajayan, O.Z. Zhou, Top Appl. Phys. 80 (2001) 391.
[3] W.H. Zhu, N. Minami, S. Kazaoui, Y.J. Kim, J. Mater. Chem. 13 (2003) 2196.
[4] G.R. Saleem, H. Ling, S. Wahyu, S.H. Hong, Nature 425 (2004) 36.
[5] H. Shimmoda, S.J. OH, H.Z. Geng, R.J. Walker, X.B. Zhang, L.E. McNeil, O. Zhou, Adv. Mater. 14 (2002) 899.
[6] P.C. Ohara, W.M. Gelbart, Langmuir 14 (1998) 3418.
[7] A. Taleb, C. Petit, M.P. Pileni, J. Phys. Chem. B 102 (1998) 2214.
[8] A.T. Ngo, M.P. Pileni, Adv. Mater. 12 (2000) 276.
[9] I. Lee, H.P. Zheng, M.F. Rubner, P.T. Hammond, Adv. Mater. 14 (2002) 572.
[10] N. Koneripalli, F.S. Bates, G.H. Fredrickson, Phys. Rev. Lett. 81 (1998) 1861.
[11] R.M. Brady, R.C. Ball, Nature 309 (1984) 225.
[12] M. Sastry, A. Gole, A.G. Banpurkar, A.V. Limaye, S.B. Ogale, Curr. Sci. 81 (2001) 191.
[13] I. Lee, J.S. Ahn, T.R. Hendricks, Langmiur 20 (2004) 2478.
[14] J. Liu, A.G. Rinzler, H.J. Dai, R.K. Hafner, P.J. Bradley, A.L. Boul, T. Iverson, K. Shelimov, C.B. Huffman, F. Rodriguez-Macias, Y. Shon, T.R. Lee, D.T. Colbert, R.E. Smalley, Science 280 (1998) 1253.
[15] L. Netzer, R. Iscovici, J. Sagiv, Thin Solid Films 100 (1983) 67.
[16] T.A. Witten, L. Sander, Phys. Rev. Lett. 47 (1981) 1400.
[17] L.M. Sander, E. Somfai, Chaos 15 (2005) 026109.
[18] W.J. Wen, K.Q. Lu, Phys. Rev. B. 55 (1997) R2100.
[19] N.D. Denkov, O.D. Velev, P.A. Kralchevsky, I.B. Ivanov, H. Yoshimura, K. Nagayama, Langmuir 20 (1992) 8419.
[20] B. Kaye, Chaos & Coplexity, VCH, Weinheim, 1993.
[21] R.C. Ball, R.M. Brady, G. Rossi, B.R. Thomson, Phys. Rev. Lett. 55 (1985) 1406.
[22] G. Daccord, J. Nittmann, H.E. Stanley, Phys. Rev. Lett. 56 (1986) 336.
[23] M. Maillard, L.M. Motte, P. Pileni, Adv. Mater. 13 (2001) 200.
[24] O. Karthaus, L. Gråsjö, N. Maruyama, M. Shimomura, Chaos 9 (1999) 308.

Characteristics of Electrodeposited Single-Walled Carbon Nanotube Film

Sung-Kyoung Kim[1], Hee-Young Choi[1], Ha-Jin Lee[2], and Haiwon Lee[1, *]

[1] *Department of Chemistry, Hanyang University, Seoul, 133-791, Korea*
[2] *Korea Basic Science Institute Jeonju Center, Jeonju, 561-756, Korea*

Thin films of chemically-functionalized single walled carbon nanotubes (SWNTs) were fabricated by using a direct current (DC) electrodeposition method. SWNTs were shortened and then functionalized with acid chloride group to combine with amine group-terminated gold substrate. The electrodeposited SWNT films were characterized by using Raman spectroscopy, attenuated total reflectance infrared (ATR/IR) spectrometry and atomic force microscopy. We demonstrated that the SWNT film was well distributed on an electrode with robust adhesion.

Keywords: Single-Walled Carbon Nanotubes, Electrodeposition, CNT Thin Film.

1. INTRODUCTION

Single-walled carbon nanotubes (SWNTs) have been considered as potential candidates for nanoscience and nanotechnology due to their outstanding properties, such as excellent mechanical property, metal-like electrical conductivity and high aspect ratio.[1] Recently, there has been an intense interest in development of thin films of carbon nanotubes on conductive surfaces for the applications as electron emission devices, large surface area electrodes and sensing devices.[2–4] The thin films of carbon nanotube could have been fabricated using various methods, such as chemical vapor deposition (CVD),[5] screen-printing,[6] electrodeposition,[7] filtration,[3] spraying,[8] self-assembling,[9] etc. We employed the electrodeposition method among them to fabricate thin films of carbon nanotube because there are several advantages in following aspects: its simple set-up, short time in processing, robust adhesion of films, no impurity, easy control of film thickness, etc. Shortly speaking of electrodeposition, carbon nanotubes suspended in a solution are forced to move toward the electrode by applying an electric field to the suspension. The carbon nanotubes collect on one of the electrodes and form a coherent deposit on it. However, the electrodeposition affected by various factors was not explained in detail in each process by now, as well as not characterized well for the products of thin films. Here, we report our observations for the electrodeposition of acid chloride-functionalized SWNTs dispersed in dimethyl formamide (DMF). The characteristics of electrodeposited SWNT films demonstrated by using various methods, such as Raman spectroscopy, attenuated total reflectance infrared (ATR/IR) spectrometry and atomic force microscopy are also described.

2. EXPERIMENTAL DETAILS

2.1. Preparation of Functionalized SWNTs

As-grown single-walled carbon nanotubes (Carbon Nanotechnologies, Inc., HiPCO SWNTs) were treated at elevated temperature and then shortened by well-known process using the oxidizing acid.[12] The shortened nanotubes were purified in a 5 M HCl solution under ultrasonic treatment, resulted in carboxylic acid-functionalized SWNTs. The COOH-SWNTs were further reacted with $SOCl_2$ to convert the carboxylic acid groups into the corresponding acid chloride at 70 °C. The black COCl-SWNTs suspension was centrifuged repeatedly at 5000 rpm for a few hours to eliminate remaining reactants and sufficiently washed with $CHCl_3$, and then dried in vaccum oven. The COCl-SWNTs were dispersed again in dimethyl formamide (DMF) with the concentration of about 0.3 mg/mL by ultrasonic treatment.

2.2. Electrodeposition of SWNTs

The method of electrodeposition was employed to deposit the acid chloride-functionalized SWNTs on amine-modified gold substrate. In the quartz cell containing the nanotube suspension, the gap distance between the gold substrate as cathode and the bare ITO as anode was fixed

at 0.8 cm by the spacer. The direct current (DC) voltage of 150 V or 50 V was applied between the two electrodes for 10 min. If it is not noted particularly, a SWNT film was fabricated at 150 V of a DC field applied for 10 min.

2.3. Characterization of the SWNT Film

Attenuated total reflectance infrared (ATR/IR) spectrometry (SensIR IlluminatIR spectrometer) equipped with a liquid nitrogen-cooled MCT detector was used to investigate the quantitative property of the SWNT film. Infrared absorption spectra were collected first on a bare gold plate as a background unit and subsequently on a SWNT film-formed gold plate which is annealed at 70 °C for 30 min. Surface property measurement of a SWNT film was conducted by a Raman confocal scanning microscope (Nanofinder 30, Tokyo Instruments, Inc.) by exciting with the 488 nm (Sapphire) radiation line. To remove an appreciable peak shift caused by the laser heating, low power of 1 mW was employed on the sample surface with the exposure time of 10 sec. Using the x, y scan stage, Raman scattered light and 2-D spectral image of a SWNT film were obtained at 1.12 cm^{-1} step intervals in a backscattering geometry using -70 °C-cooled CCD for the phonon detection.

3. RESULTS AND DISCUSSION

Figure 1 shows single walled carbon nanotubes (SWNTs) before and after shortening process. The acid chloride-functionalized SWNTs (COCl-SWNTs) had no iron catalytic particles generated in the HiPCO process. The length of highly-entangled, raw SWNTs (usually >10 μm) was reduced to less than 1 μm with a rod-like shape. We found that the crystallinity of SWNTs was conserved even after shortening process using the oxidizing acid as shown in Figure 1(b).

Dimethyl formamide (DMF) has been known as a good solvent in dispersing SWNTs. DMF has the dielectric constant of about 37 at 25 °C that is high enough to be applied to electrodeposition process. DMF, here, was used as a solvent in the COCl-SWNT suspension without the addition of ionic compounds. SWNTs are a good candidate for an electrodeposition and movable in DMF solution because they are easily charged under an electric field due to the metal-like properties of carbon nanotubes. Figure 2 suggests the electrodeposition process of COCl-SWNT in dimethyl formamide. When an electric field was applied to the SWNT suspension, the SWNT aggregates were produced immediately in the suspension. The COCl-SWNTs, however, were well dispersed in dimethyl formamide (DMF) before applying an electric field. Since the stability in dispersion usually decreases with increasing ionic concentration, it is suggested that chloride ions are produced by dissociating from acid chloride groups on SWNTs under the influence of DC field.[13] A good leaving
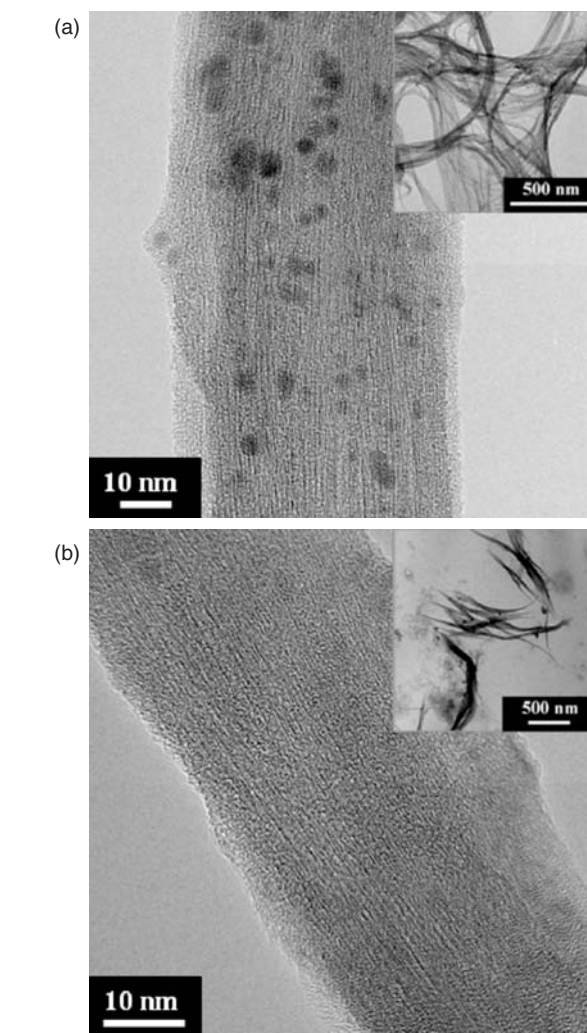

Fig. 1. Transmission electronic micrographs of a bunch of (a) raw SWNTs and (b) acid chloride-functionalized SWNTs. The insets show each TEM image in a low resolution.

group of Cl$^-$ in COCl-SWNT was simply confirmed by adding a small amount of a silver ion to SWNT suspension. While the sediment of AgCl was produced especially near the anode during applying an electric field, the sediment in SWNT suspension was not observed due to the absence of Cl$^-$ ion under no influence of an electric field. In the middle space between two electrodes, the polarized SWNTs under an electric field are stabilized in charge due to the compensation of chloride ions as shown in Figure 2 (A: middle space).[14] The SWNTs near both electrodes migrated with a high speed toward the electrodes, caused by a strong charge interaction. On the cathode terminated with amine groups, a uniform SWNT film was formed with a covalent bond as shown in Figure 2 (B: cathode). After prolonged deposition time, the coagulated SWNTs were difficult to be deposited on the electrode because of its irregular shape.[15] The dissociated chloride ions, Cl$^-$, migrate toward the positive electrode. The increase in the concentration of chloride ions near the anode resulted in
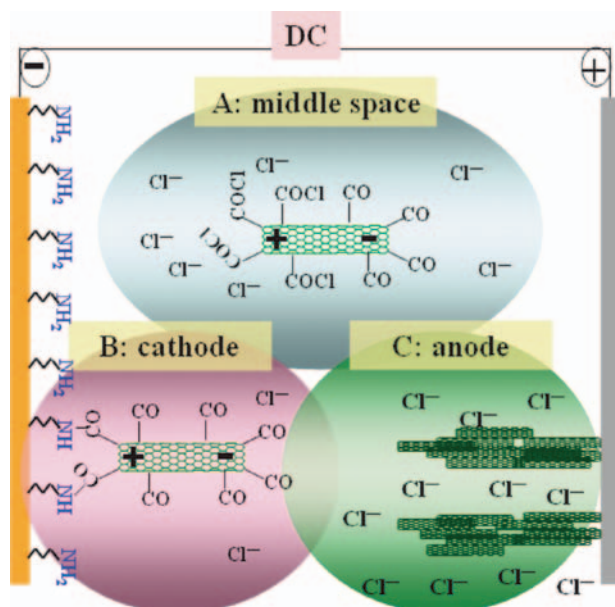
Fig. 2. Schematic view of the electrodeposition process of COCl-SWNTs in dimethyl formamide.

Fig. 3. (a) Scanning electron micrographs of a SWNT film formed on NH_2-functionalized gold electrode by applying an electric field at 150 V for 10 min. (b) Infrared absorption spectra of the SWNT films (A) physisorbed, (B) physisorbed and subsequently ultrasonic-irradiated for 3 min, (C) chemisorbed, and (D) chemisorbed and subsequently ultrasonic-irradiated for 3 min. The films were obtained either on a bare gold (physisorption) or on a cysteamine-modified gold (chemisorption) by applying a DC field of 50 V for 10 min. Band around 1500 cm^{-1} corresponds to the stretch mode of the aromatic carbon–carbon bond.

the assembly of SWNTs in a bundle as shown in Figure 2 (C: anode). The assembly of SWNTs also comes from the strong electric field analogous to the previous report.[14]

The acid chloride-functionalized SWNTs (COCl-SWNTs) were deposited on the NH_2-modified gold substrate by applying a DC field at 150 V or 50 V for 10 min. Figure 3(a) presents the densely deposited, uniform SWNT film obtained at a DC field of 150 V. The formation of a SWNT film in electrodeposition depends on various factors, such as concentration of SWNT, strength of electric field, nature of electrolyte, etc. The thickness of SWNT film was controlled with a variation in the concentration of SWNT, the strength of electric field and the applying time. The aggregation of SWNTs, however, has occurred seriously at higher concentration (>0.8 mg/ml at 150 V) of SWNTs in DMF, resulting in the SWNT film with low uniformity. The increase in the concentration of a chloride ion on anode made SWNTs aggregated into bundles which were attached on anode with poor adhesion. On the contrary, COCl-SWNTs were deposited robustly on the cathode either of a bare gold or of a gold modified with cysteamine. In addition, the uniform films of SWNTs were obtained on both of the gold cathodes. The adhesion of the films in both cases was strong, but showing a different stability under the influence of ultrasonication. To investigate adhesion property of the electrodeposited SWNT film, physisorbed and chemisorbed SWNT films were fabricated at 50 V of an electric field applied for 10 min on a bare gold and on a cysteamine-modified gold, respectively. Then, ultrasonication was applied to both of the films for 3 min. The infrared adsorption spectra in Figure 3(b) were obtained on the samples to investigate the quantity of SWNTs in the films. In this work, the most distinct
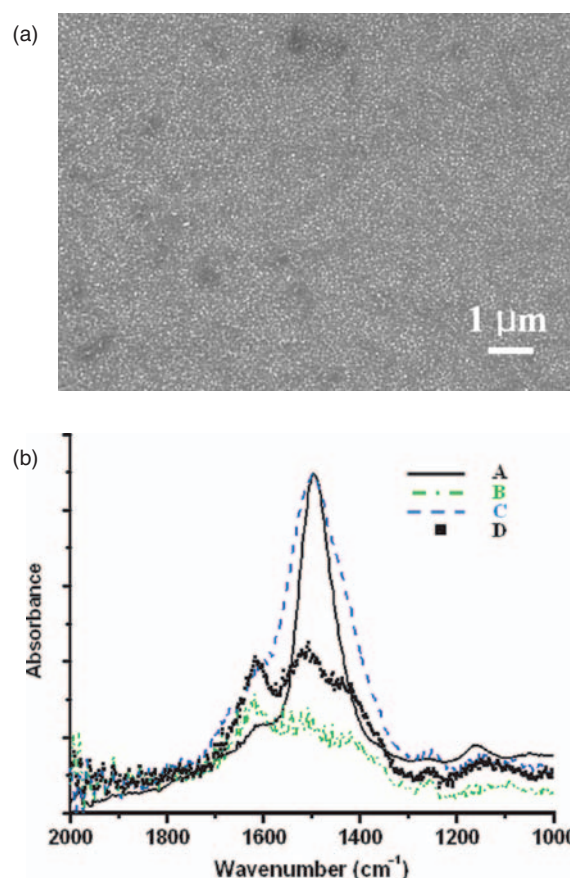
peak in the spectra of the SWNT films was the absorption band of the stretch mode of the aromatic carbon–carbon bond observed at about 1500 cm^{-1}. Although the peak intensity of the physisorbed SWNT film on a bare gold was similar with that of the chemisorbed SWNT film on a cysteamine-modified gold, the intensity of the physisorbed film was lower than that of the chemisorbed film after ultrasonication for 3 min. The result shows that physically adsorbed COCl-SWNTs on a bare gold are easily detached compared to chemically adsorbed COCl-SWNTs on NH_2-terminated gold under ultrasonication.

To characterize the electrodeposited SWNT film in detail, we introduced tapping-mode atomic force microscope (AFM) in imaging the SWNT film. The results induced needle-like topography from which one can be confused as if SWNTs were vertically aligned on a substrate. The needle-like image comes from the particular scanning system of AFM, by which the AFM tip is vibrated perpendicular to the substrate in tapping mode
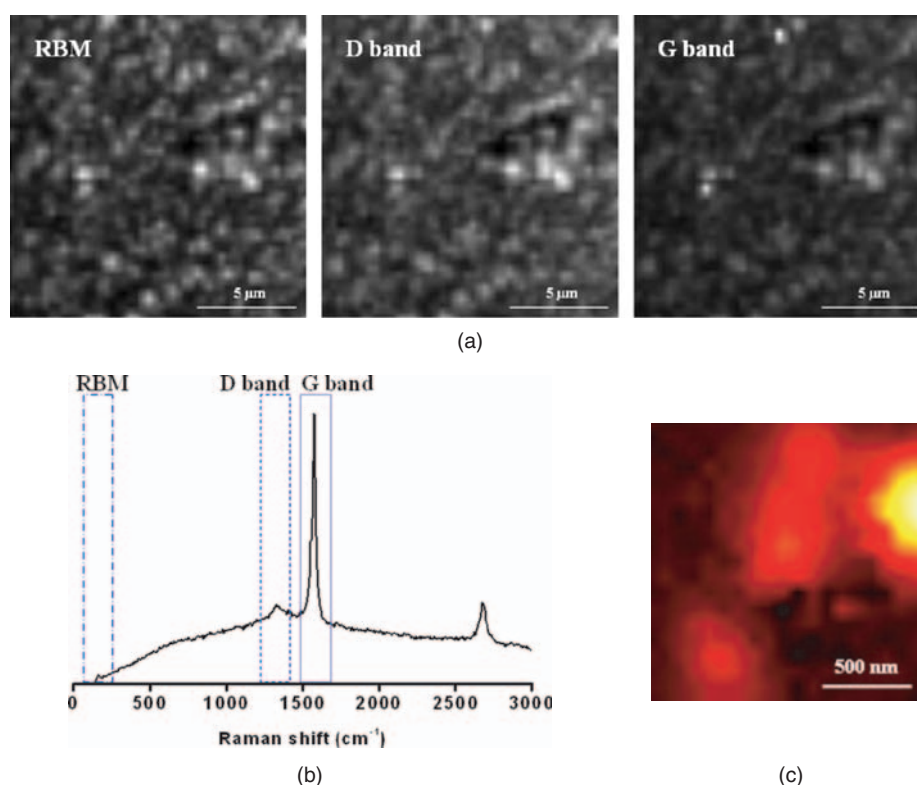
(a)

(b)

(c)

Fig. 4. (a) Raman spectral images of a SWNT film deposited on gold substrate. The contrast in the images presents the local intensity of the RBM mode (172 cm^{-1}), Raman D band (1332 cm^{-1}) and G band (1578 cm^{-1}), (b) Raman scattering spectrum for the SWNT film and (c) the magnified Raman spectral image of the film at Raman G band (1578 cm^{-1}).

or in non-contact mode. The densely packed SWNTs and the big differences in the height of the structure ($> \sim100$ nm) also play a key role to present a needle-like topography in AFM image. As an another trial, the distribution of SWNTs in a SWNT film was surveyed by imaging the film using Raman spectroscopy which provides chemical and structural information of a sample. Figure 4(a) shows confocal Raman images (15×15 μm^2) recorded by scanning a SWNT film with the focused laser. The images were acquired by detecting intensity of the RBM mode (172 cm^{-1}), Raman D band (1332 cm^{-1}) and G band (1578 cm^{-1}), respectively, upon laser excitation at 488 nm. From the contrast of the images, it was found that a SWNT film was composed entirely of the SWNTs with defect sites. Figure 4(b) shows the representative Raman scattering spectrum for the SWNT film, which provides typical four main Raman shifts of SWNT: RBM (~100–300 cm^{-1}), Raman D band (~1300 cm^{-1}), G band (~1592 cm^{-1}), and G′ band (~2600 cm^{-1}).[16] The frequency of the RBM is very sensitive to the tube diameter. The isolated tubes are concerned the following equation, ν (cm^{-1}) = A/d (nm), where ν is the RBM frequency, **d** SWNT diameter, **A** proportionality constant. The diameters of the electrodeposited SWNTs (1.2 nm–1.4 nm), however, were well agreed with those of the typical HiPCO SWNTs (0.8 nm–1.4 nm) when applying various relations between the RBM frequency

and the inverse of the SWNT diameter.[17–20] The magnified Raman image at G band (1578 cm^{-1}) of the SWNT film is shown in Figure 3(c), in which the high intensity of Raman G band (showing red and deep yellow colors) could be observed for the SWNTs even after shortening process and subsequent electrodeposition process. The G band originating from the tangential oscillations of the carbon atoms in the nanotube defines ordered carbons with metallic or semiconducting helicity. Therefore, the electrodeposited SWNT films were demonstrated to have the property of electrical conductivity which is very important for the future applications of SWNT films.

4. CONCLUSION

In conclusion, we demonstrated well distributed SWNT films using DC electrodeposition method. The characterization of the SWNT film was performed using Raman spectroscopy, attenuated total reflectance infrared (ATR/IR) spectrometry, atomic force microscopy. As a result, the properties of adhesion and electrical conductivity have drawn the possibility of a SWNT film applied to potential applications like electron emitters and large surface area electrodes. Deep understanding for the electrodeposition of SWNTs would contribute to promoting the properties of a SWNT film such as uniformity, adhesion, density, alignment, etc. The simple fabrication of

a SWNT film using DC electrodeposition would enable SWNTs to be integrated into electronic devices, especially electron emission devices.

References and Notes

1. R. H. Baughman, A. A. Zakhidov, and W. A. de Heer, *Science* 297, 787 (**2002**).
2. S. J. Oh, J. Zhang, Y. Cheng, H. Shimoda, and O. Zhou, *Appl. Phys. Lett.* 84, 3738 (**2004**).
3. Z. Wu, Z. Chen, X. Du, J. M. Logan, J. Sippel, M. Nikolou, K. Kamaras, J. R. Reynolds, D. B. Tanner, A. F. Hebard, and A. G. Rinzler, *Science* 305, 1273 (**2004**).
4. J. Sippel-Oakley, H. T. Wang, B. S. Kang, Z. Wu, F. Ren, A. G. Rinzler, and S. J. Pearton, *Nanotechnology* 16, 2218 (**2005**).
5. Z. P. Huang, D. L. Carnahan, J. Rybczynski, M. Giersig, M. Sennett, D. Z. Wang, J. G. Wen, K. Kempa, and Z. F. Ren, *Appl. Phys. Lett.* 82, 460 (**2003**).
6. K. Nishimura, Z. Shen, M. Fujikawa, A. Hosono, N. Hashimoto, S. Kawamoto, S. Watanabe, and S. Nakata, *J. Vac. Sci. Technol. B* 22, 1377 (**2004**).
7. Y. Abe, R. Tomuro, and M. Sano, *Adv. Mater.* 17, 2192 (**2005**).
8. C. Bower, O. Zhou, W. Zhu, A. G. Ramirez, G. P. Kochanski, and S. Jin, *Mater. Res. Soc. Symp. Proc.* 593, 215 (**2000**).
9. O. J. Lee, S. H. Jeong, and K. H. Lee, *Appl. Phys. A* 76, 599 (**2003**).
10. Q. Chen and L. Dai, *Appl. Phys. Lett.* 76, 2719 (**2000**).
11. J. C. Hulteen, D. A. Treichel, M. T. Smith, M. L. Duval, T. R. Jensen, and R. P. Van Duyne, *J. Phys, Chem. B* 103, 3854 (**1999**).
12. J. Liu, A. G. Rinzler, H. Dai, J. H. Hafner, R. K. Bradley, P. J. Boul, A. Lu, T. Iverson, K. Shelimov, C. B. Huffman, F. Rodriguez-Macias, Y. S. Shon, T. R. Lee, D. T. Colbert and R. E. Smalley, *Science* 280, 1253 (**1998**).
13. O. O. Van der Biest and L. Vandeperre, *J. Annu. Rev. Mater. Sci.* 29, 327 (**1999**).
14. P. V. Kamat, K. G. Thomas, S. Barazzouk, G. Girishkumar, K. Vinodgopal, and D. Meisel, *J. Am. Chem. Soc.* 126, 10757 (**2004**).
15. Y. Abe, R. Tomuro, and M. Sano, *Adv. Mater.* 17, 2192 (**2005**).
16. A. Jorio, R. Saito, J. H. Hafner, C. M. Lieber, M. Hunter, T. McClure, G. Dresselhaus, and M. S. Dresselhaus, *Phys. Rev. Lett.* 86, 1118 (**2001**).
17. N. Anderson, A. Hartschuh, S. Cronin, and L. Novotny, *J. Am. Chem. Soc.* 127, 2533 (**2005**).
18. S. Rols, A. Righi, and J. L. Sauvajol et al, *Eur. Phys. J. B* 18, 201 (**2000**).
19. X. Zhang, W. Zhang, L. Liu, and Z. X. Shen, *Chem. Phys. Lett.* 372, 497 (**2003**).
20. A. M. Rao, J. Chen, E. Richter, U. Schlecht, P. C. Eklund, R. C. Haddon, U. D. Venkateswaran, Y.-K. Kwon, and D. Tomanek, *Phys. Rev. Lett.* 86, 3895 (**2001**).

RESEARCH ARTICLE

Vertical Alignment of Single-Walled Carbon Nanotube Films Formed by Electrophoretic Deposition

Sung-Kyoung Kim[a], Haiwon Lee*[a], Hirofumi Tanaka[b], Paul S. Weiss[c]

[a]   Department of Chemistry, Hanyang University, Seoul 133-791, Korea

[b]   Institute of Molecular Science, Okazaki 444-8787, Japan

[c]   Departments of Chemistry and Physics, The Pennsylvania State University, University Park, PA 16802, USA

E-mail: haiwon@hanyang.ac.kr

Fax: (+82) 2-2296-0287

(carbon nanotube, alignment, electrophoretic deposition, atomic force microscopy, sonication)

Single-walled carbon nanotubes (SWNTs) have attracted much attention because of their amazing properties, such as excellent mechanical strength, metal-like electrical conductivity and extreme aspect ratios.[1] To apply such SWNTs to a plethora of technologies, many researchers have tried to develop methods to control and to align SWNTs.[2] Chemical processing of as-grown SWNTs has allowed SWNTs to be controlled in length, purified, modified with functional groups, dispersed in desired solvents and eventually aligned on substrates.[2c,3] Moreover, various methods for aligning chemically functionalized SWNTs, such as self-assembly,[4] exploitation of hydrophilic/hydrophobic interactions[5] and electrochemistry,[6] have also been introduced because of their simplicity at ambient temperature and their applicability to relatively large areas. Using these controllable processes, horizontally aligned and micropatterned carbon nanotubes have been formed to apply carbon nanotubes as active components in carbon-nanotube-based devices.[5,7] There have only

1

been limited studies of vertically aligned and micropatterned carbon nanotubes, however, especially by post-synthesis treatments rather than by direct growth methods like chemical vapor deposition (CVD).[8] For instance, functionalized SWNTs have been believed to be vertically assembled on modified substrates in analogy to the self-assembly of active surfactant molecules such as alkanethiols and organosilicons. Even though the shapes of SWNTs, which usually disperse as bundles in solution, resemble the long-chain molecules available for ordering into self-assembled monolayers, it would be difficult for SWNT bundles to align spontaneously normal to the surface due to their great lengths, irregular size distributions in suspension and low density on modified surfaces.

Recently, a direct current (DC) electrophoretic deposition method has been applied to form SWNT films efficiently on substrates, providing high surface coverages and short assembly times.[9] The alignment of SWNTs was also performed by applying an electric field as an external force to SWNT suspensions, which made length-controlled SWNTs easy to polarize and therefore aligned by dielectrophoresis in the direction of the electric field between two metallic electrodes placed on either a flat insulator or semiconductor.[10] Highly densified SWNT films formed on a flat electrode by electrophoretic deposition, however, are randomly aligned laterally and also compressed by a strong electric field,[9b] resulting in almost flat films; their random orientation limits their technological applications. Here, we report SWNT films electrodeposited on flat gold electrodes and the first observations of their vertical alignment over a large area.

For liquid-solid systems, ultrasonic irradiation has been used in cleaning processes, mixed phase reactions, sono-catalysis, enhancement of mass transport, etc.[11] Dispersing and shortening carbon nanotubes have also employed ultrasonic treatment.[3a,12] Acoustic cavitation by ultrasonic waves produces turbulent flow and shock waves that cause enormous

concentration of energy, sufficient to make a solid unstable in liquid. It is demonstrated here that controlled ultrasonication enhances the orientation of electrodeposited SWNT films.

Highly entangled, raw SWNTs were shortened to ease control, then chemically functionalized and eventually dispersed in dimethyl formamide (DMF). The lengths and diameters of the SWNT bundles after the shortening process were typically smaller than 1 μm (predominantly 600 ± 100 nm) and 50 nm (predominantly 35 ± 10 nm), respectively, which were confirmed by atomic force microscopy and scanning electron microscopy. (Figure S1) The shortened carboxylic-acid-functionalized SWNTs (SWNTs-COOH) were further modified with $SOCl_2$ into acyl-chloride-functionalized SWNTs (SWNTs-COCl) to enable chemical bonding of the SWNTs with amine-functionalized gold electrodes, which not only enhanced adhesion[13] but reduced the contact resistance between the SWNTs and the electrodes.[14] Figure 1(a) shows a simple schematic of a setup for electrophoretic deposition and actual cells containing a SWNT suspension before and after applying an electric field between two electrodes separated by a 0.8 cm gap. Figure 1(b) shows the resulting representative, uniform SWNT film electrodeposited on the cathode at a DC voltage of 150 V for 10 min.
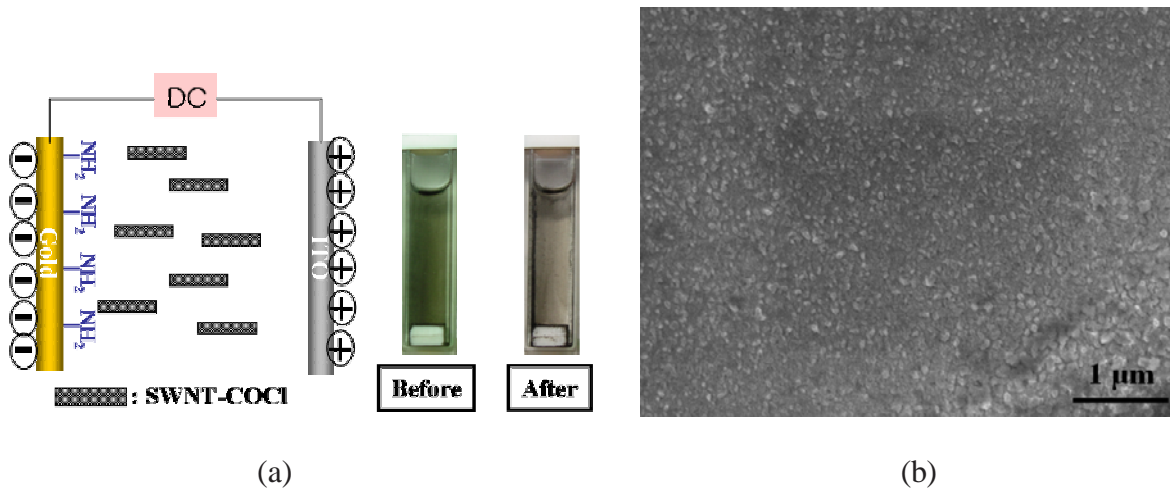
(a)	(b)

Figure 1. (a) Simple schematic of a setup for electrophoretic deposition of SWNTs-COCl on gold electrodes functionalized with self-assembled monolayers terminating in amine groups using a DC field and the electrophoretic cells containing a SWNT suspension before and after applying a DC field. (b) Scanning electron micrograph of a SWNT film formed on a gold electrode by applying an electric field at 150 V for 10 min.

When applying a DC electric field using the setup shown in Figure 1(a), SWNTs migrated along with the convection flow of the suspension in the space between the two electrodes in the direction of the electric field. High-speed migration of SWNTs was observed near both electrodes, where the electric field is very strong. SWNT aggregates also began to appear in the suspension. After a few minutes, the black suspension became transparent due to the deposition of SWNTs on both electrodes and the sedimentation of coagulated SWNTs. The serious coagulation of SWNTs happened immediately after applying voltages above 300 V. When applying an electric field, the coagulation of SWNTs rose in the solution in any case but in different degree with applied voltages. Below 50 V, the movement of SWNTs was not

4

visible in the cell and thus poor films were formed because of the weak electric field. The coagulation became gradually serious as the deposition time increased.

While a robust film of SWNTs was formed on the cathode, assembled bundles of SWNTs, which were aligned parallel to the direction of electric field, as reported by Kamat et al.,[9c] were formed on the anode and then detached after a few minutes. In our electrophoretic deposition system, a small amount of $SOCl_2$ was included in the SWNTs-COCl/DMF suspension (pH 7 ~ 7.5). The value of the pH could be controlled through the separation process of $SOCl_2$ using centrifuge after completion of the modification of SWNT-COOH into SWNT-COCl. At the point of zero charge (pH 7 ~ 7.5 in this case) which differs from the iso-electric point, the concentration of negatively and positively charged surface groups is equal because the suspension was very stable. Dettlaff-Weglikowska et al. demonstrated that chemical modification of HiPco SWNTs by $SOCl_2$ largely enhanced the electrical conductivity of SWNTs due to formation of SWNT/$SOCl_2$ charge-transfer complexes within the intercalated ropes.[15] The $SOCl_2$-modified HiPco SWNTs showed the electrical conductivity 5 times higher than that of pristine HiPco SWNTs. This transition from semiconducting to metallic behavior enabled the enhancement of the alignment of SWNTs in the electrophoretic deposition. On the other hand, the chloride ion (Cl^-) leaving group in SWNTs-COCl affected the electrophoretic behavior in which the increase in concentration of the chloride ion near the anode after applying an electric field resulted in coagulated SWNT bundles. The chloride ion near the anode was simply confirmed by adding $AgNO_3$ to the SWNT suspension (Ag^+ ions remove Cl^- by precipitation as AgCl). The coagulated bundles adhered only weakly to the anode because of their bulky sizes and irregular shapes.[9b,16]

Figure 2(a) is a magnified image of Figure 1(b) that shows densely-deposited SWNTs, which appear compressed. It was found that the morphology of SWNT films was significantly changed for different gap sizes between anode and cathode. Gap sizes within a few mm at

concentrations of about 0.3 mg/ml resulted in horizontally and randomly aligned SWNT films that we attribute to SWNT coagulation both by the electric field in a narrow gap between two electrodes and by high concentrations of SWNTs. (Figure S2) In contrast, shortened SWNTs electrodeposited using a broad gap (more than a few mm) appeared to get stuck normal to the electrode. The alignment of SWNTs by electric fields has been demonstrated by many researchers.[10] The electric field induces a dipole moment in a carbon naotube by which the dipole experiences a torque. This torque is regarded as a driving force for the alignment of the nanotubes in the field direction. However, the planar electrodes facing with each other will have fringing fields toward the edges of the electrodes, which are very nonuniform especially as the gap becomes narrow. Thus, broad gap is more useful for SWNTs to be aligned normal to the electrode. The effect of gap distance, however, is not independent on the concentration of the suspension and the field strength. Higher concentrations (>0.5 mg/ml) gave rise to serious coagulation of SWNTs even in the broad gap, resulting in the poor SWNT films. When applying an electric field, the deposition always competes against the coagulation due to the imbalance between van der Waals' attraction and electrostatic double-layer repulsion.[9b] SWNT coagulates showed the characteristics of low adherence on the electrode due to their irregular shape. In contrast, lower concentrations (<0.1 mg/ml) produced low coverage deposition on the electrode. From our observations, the lengths of SWNT bundles also affect the morphology of the SWNT films. We suggest that each SWNT bundle is aligned parallel to the electric field and is driven towards, compressed against and deposited normal to the electrode. Figure 2(a) indicates that ultimately the compressed SWNT bundles may be aligned by applying an external force.

Figures 2(b)-2(d) show the varying film morphology found after ultrasonication of the SWNT film for different times in DMF. A densely packed, unidirectionally aligned SWNT film was obtained after ultrasonication for 2 min as shown in Figure 2(b). Yokoi et al.

reported dynamic reassembly of self-assembled peptide nanofiber scaffolds through ultrasonication.[17] Weak forces like hydrogen bonds and hydrophobic interactions are easily broken by applying ultrasonic energy, compared to stronger covalent peptide bonds. They suggested that ultrasonication allowed reassembly of the mechanically dissembled individual peptide chains. We suggest here that densely deposited and compressed SWNT bundles, which adhere via hydrophobic interactions, are annealed and aligned by ultrasonication. With increasing ultrasonication time, smaller SWNTs with narrower diameter distributions appeared on the electrode due to desorption of bulky SWNTs, as shown in Figures 2(c) and 2(d). Furthermore, we found that the SWNT bundles were well distributed with uniform space between them and were mostly aligned normal to the surface after 3 min ultrasonication, as shown in the 45° tilt SEM image of Figure 2(e). This method for aligning SWNTs normal to the surface is comparable to chemical vapor deposition (CVD) or screen printing methods by which SWNT films have been fabricated predominantly to date. The arrow in the inset of Figure 2(c) indicates the "three-bundles-folded structure" that can be observed only in standing structures. The structures of SWNTs in electrodeposited SWNT films were surveyed using Raman spectroscopy; representative shifts observed included the Raman G band (1592 cm^{-1}) and D band (1346 cm^{-1}), typical of SWNTs. (Figure 2(f)) The inset in Figure 2(f) shows the observed radial breathing mode (RBM) frequency range of 161 − 202 cm^{-1}, which corresponds to tube diameters ranging from 1.4 to 1.1 nm and agrees well with those of typical HiPCO SWNTs (1.4 − 0.8 nm).[18]
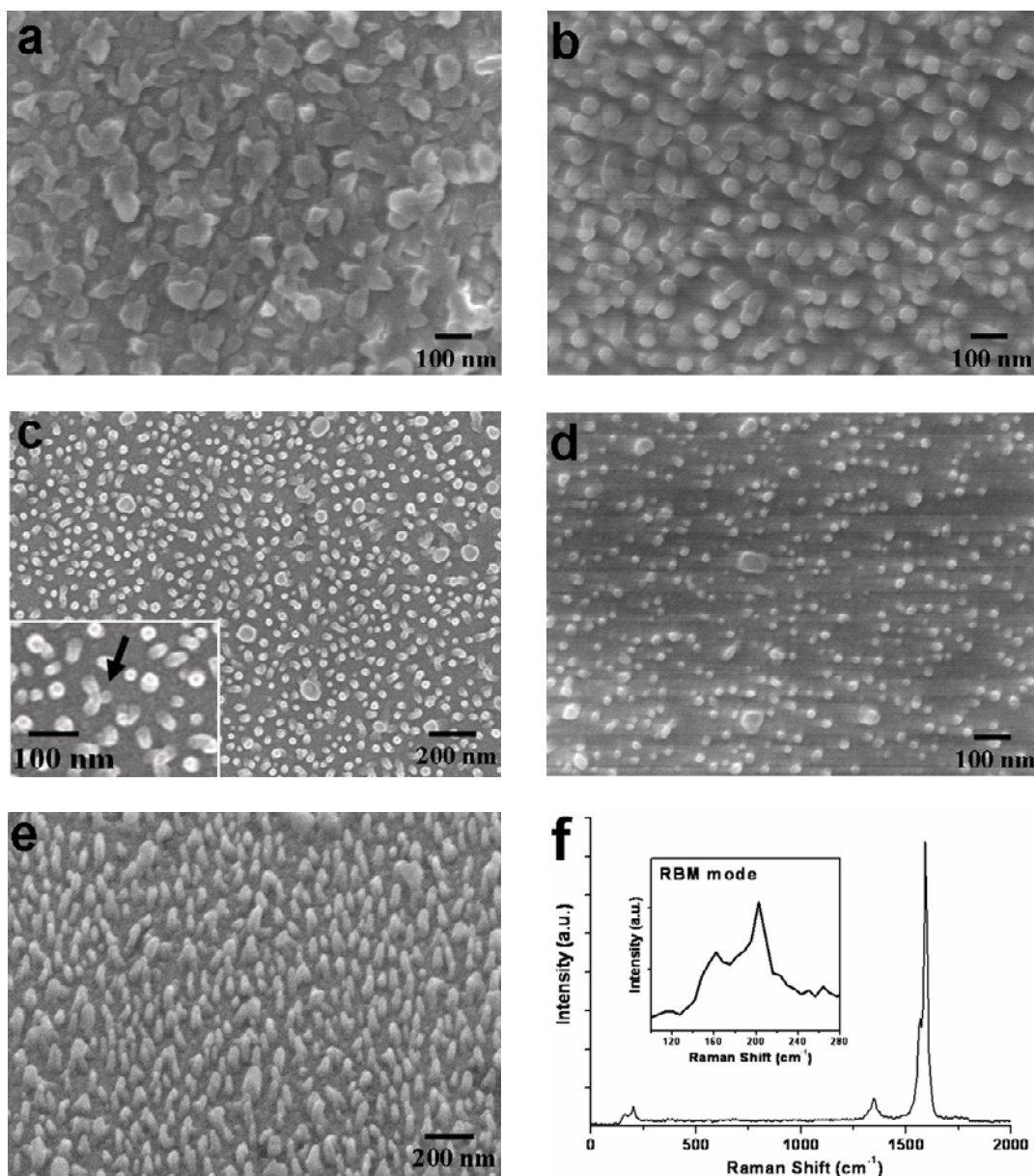
Figure 2. (a) Scanning electron micrographs of a SWNT film formed on a gold electrode by applying an electric field at 150 V for 10 min. The SWNT film was ultrasonicated (b) for 2 min, (c) for 3 min and (d) for 5 min in HPLC-grade dimethyl formamide. (The inset of Figure 2(c) is a magnified image of Figure 2(c) and the arrow indicates the three-bundles-folded structure.) (e) 45° tilt picture of Figure 2(c) and (f) Representative Raman spectrum for the electrodeposited SWNT film. (The inset of Figure 2(e) shows a Raman spectrum in the radial breathing mode region)

8

Figure 3(a) shows the extent of detachment of SWNT bundles with ultrasonication time. The absorbance intensity at 1500 cm^{-1} for SWNT films decreases gradually with increasing ultrasonication time. Although the SWNT film deposited at 150 V for 10 min presented higher intensity (that is, higher density) than the film at 50 V for 10 min, the absorbance intensity for both of the films decreased at a comparable rate with increased ultrasonication time. Figure 3(b) shows that a great number of SWNT bundles (>250 bundles/µm^2) with average diameters of about 27 nm were exposed to the surface after 3 min ultrasonication. In fact, controlling the density of carbon nanotubes on surfaces is very important for many applications, especially for carbon-nanotube-based fuel cell electrodes with large surface areas and for displays. However, the number of exposed SWNT bundles was small (about 150 ± 20 bundles/µm^2) for SWNT films ultrasonicated for 0 or 2 min, presumably because of the shielding effects of the relatively large size SWNT bundles. For SWNT films ultrasonicated for 5 min, the surface density of SWNT bundles was reduced by desorption of SWNT bundles.

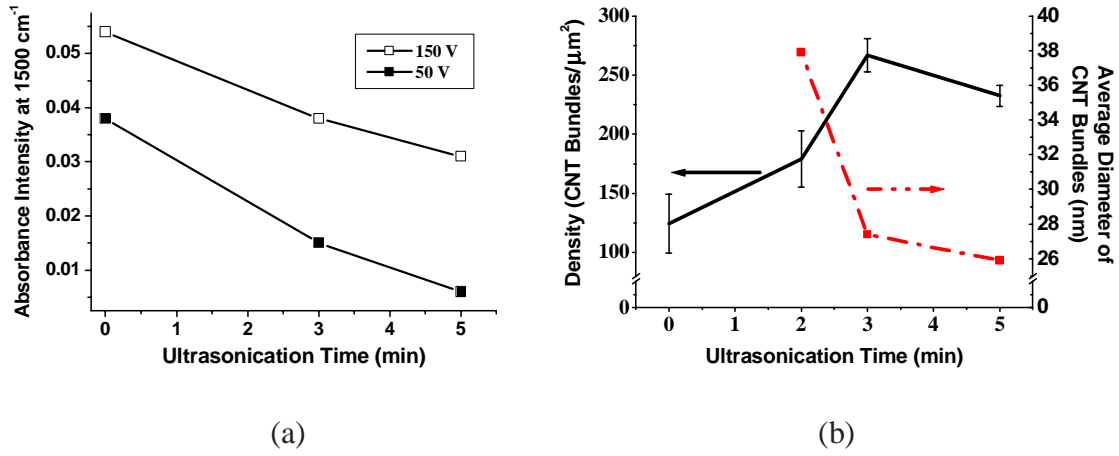(a)   (b)

Figure 3. (a) Trends in infrared absorbance of SWNT films deposited at 150 V and at 50 V vs. ultrasonication time. The infrared absorbance was obtained from attenuated total reflectance spectra (SENSIR IlluminatIR spectrometer) of the SWNT films. The band at 1500 cm^{-1} corresponds to the stretch mode of the aromatic carbon-carbon bond. (b) The variation of SWNT density (CNT bundles/μm^2) obtained from counting CNT bundles and of average diameter of SWNT bundles (nm) with ultrasonication time. The solid line shows the variation in density and the dashed line the average diameter.

By comparing images obtained by different and complementary methods (Figures 2 and 4), we have found that the morphology of the SWNT films obtained by tapping mode atomic force microscopy (TM-AFM) can be misleading. Although Figure 2(a) shows no SWNT bundles aligned normal to the surface, 3-dimensional (3D) displays of TM-AFM topography images of the film appeared to show needle-like protrusions, which can be mistaken for vertically aligned SWNTs. In addition, 3D displays of AFM images are usually presented with distorted perspective, compressed in the laterally scanned xy plane and expanded in the z direction, normal to the surface. In fact, there have been several previous reports that included needle-like 3D TM-AFM images as evidence of vertically aligned

carbon nanotubes through post-synthesis treatments including self-assembly and electrophoretic methods.[2b,4b,19] Based on the results shown here, we do not believe that AFM measurements alone are sufficient to indicate alignment normal to the surface. When we fabricated carbon nanotube films (SWNT-COCl) on amine-functionalized Si substrates, we were able to obtain SWNT bundles aligned normal to the surface as determined from *both* SEM and TM-AFM images. Figures 4(a) and 4(b) show 2D and 3D displays of AFM images (XE-100, PSIA Inc., Korea) of self-assembled SWNT films with scan sizes of 10x10 μm^2 and 2x2 μm^2, respectively. Previous reports typically showed what appeared to be needle-like protrusions of nanotubes in 3D displays of AFM images (typically with scan areas of 10x10 μm^2), similar to Figure 4(a) (3D display). The 2D display of Figure 4(a), however, shows randomly and horizontally aligned SWNTs and some particles, as confirmed in the corresponding SEM image recorded at approximately the same scale (Figure 4(d)). Likewise, TM-AFM images Figure 4(b) and corresponding SEM images Figure 4(e) were both recorded with scan areas of 2x2 μm^2 to compare with Figure 4(c), which was obtained from scanning the same area for the vertically aligned SWNT films scanned with TM-AFM and shown in Figure 2(e). It was found that the 2D and 3D displays of TM-AFM images of the vertically aligned SWNT film (Figure 4(c)) were much different than those of self-assembled SWNT films. Although the 2D displays of TM-AFM images of the vertically aligned SWNT film (Figure 4(c)) show only dot-like structures, those of the self-assembled SWNT films (Figure 4(b)) show structures similar to those of Figure 4(a). This means that the 3D displays of AFM images do not necessarily represent the structure of the surface, and therefore should not be used as diagnostics of nanotube alignment.

In addition, we found that TM-AFM images of the vertically aligned SWNT film were often distorted. We posit that this originates from contact between the flexible SWNT bundles with the hard AFM tip during operation in tapping mode as suggested in Figure 4(f). Soft materials like proteins have also been shown to yield distorted images because of interactions between the AFM tip and the flexible samples.[20] Further, the vertically aligned SWNT bundles appeared to be nearly in contact with one another in TM-AFM images (e.g., Figure 4(c)) even though there were uniform spaces (several tens of nm) between them as shown in Figure 2(e). This originates from the convolution of the tip and sample geometries, which does not allow an AFM tip to penetrate into such narrow spaces on the vertically aligned SWNT films. (Figure S3) Therefore, the apparent depths and widths of the spaces are underestimates of their true values due both to interactions of the AFM tip with the SWNT bundles and to the convolution of the tip and sample geometries.
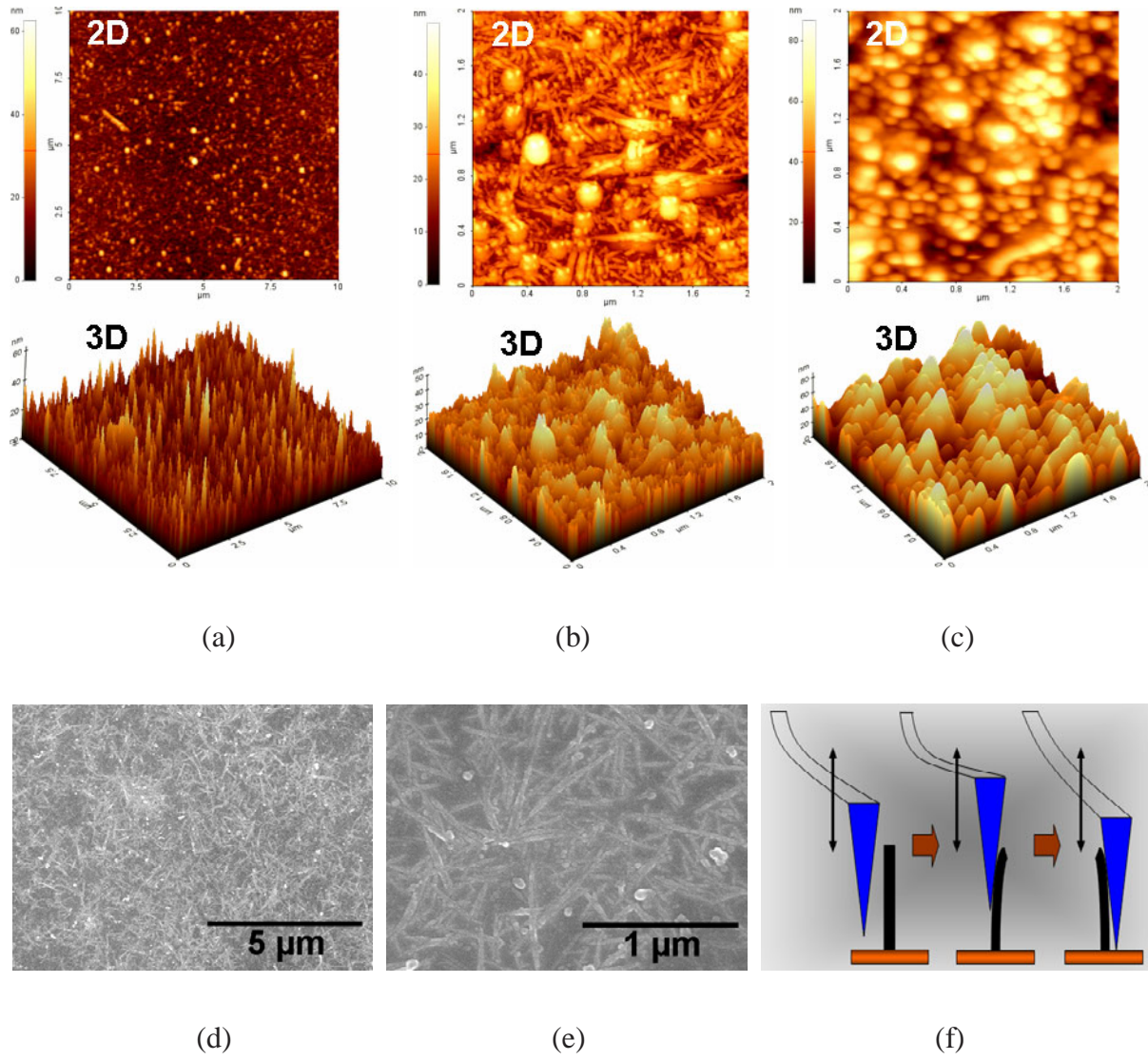
Figure 4. 2D and 3D tapping mode AFM images of SWNTs-COCl self-assembled on amine-functionalized Si substrates with scan sizes of (a) 10x10 µm^2 and (b) 2x2 µm^2, and of (c) vertically aligned SWNT film (scan size, 2x2 µm^2) shown in Figure 2(e). SEM images of the self-assembled SWNT films with a scan size of (d) about 10x10 µm^2 and (e) about 2x2 µm^2. (f) Schematic showing the interaction between a hard AFM tip and a flexible vertically aligned SWNT bundle while scanning with tapping mode AFM.

In conclusion, we have introduced a novel and simple method for fabricating large area, vertically aligned SWNT films. Ultrasonic treatment after electrophoretic deposition enables randomly deposited SWNT bundles to be aligned normal to the electrode, distributed over large areas. This simple method may prove useful in the fabrication of carbon nanotube-based electron emission devices or fuel cell electrodes. We have confirmed the structures and alignment of the SWNT bundles using both SEM and TM-AFM imaging.

Experimental Section

As-grown single-walled carbon nanotubes (Carbon Nanotechnologies, Inc., HiPco SWNTs) were treated at elevated temperature and then shortened by processing using oxidizing acid.[12] The collected SWNTs after filteration were weighed and then immersed into $SOCl_2$ at 70℃ for 24 hr to convert the carboxylic acid groups into the corresponding acyl chloride. After completion of the reaction, the black SWNTs-COCl suspension was centrifuged at 5000 rpm for a few hours to eliminate remaining reactants (the upper solution), and then diluted with dimethylformamide (DMF, 0.001% water). After repeating the process a few times, we could obtain the SWNTs-COCl/DMF solution with a small amount of $SOCl_2$ (pH = 7 ~ 7.5). A gold-coated substrate, obtained by thermal evaporation with an adhesive layer of chromium on Si/SiO_2, was immersed in 5 mM cysteamine/ethanol solution for 20 min to obtain a cysteamine self-assembled monolayer. The electrophoretic deposition was conducted in a quartz cell (1 $\times$ 1 $\times$ 2.5 cm^3) containing two electrodes separated by Teflon spacers. After deposition process, the electrodes were rinsed thoroughly with DMF and ethanol. Ultrasonic irradiation (Branson 2510 sonicator bath operating at 40 KHz) was engaged to induce reassembling of nanotube bundles in the SWNT film. The SWNTs-deposited electrode was immersed in the beaker containing DMF followed by placing the beaker in the sonicator bath. After sonication, the electrode was rinsed again with DMF and ethanol and then dried under the nitrogen stream. The SWNT film was characterized by using a Raman confocal scanning microscope (Nanofinder 30, Tokyo Instruments, Inc) by exciting with the 488 nm (Sapphire) radiation line. To remove an appreciable

peak shift caused by laser heating, low power (1 mW) was employed on the sample surface with an exposure time of 10 sec. To fabricate a SWNT film using self-assembly, the surface of an oxidized silicon wafer (SiO_2/Si(100)) was treated with (3-aminopropyl)triethoxysilane for 1 h in solution. The amine group-terminated Si substrate was exposed to the SWNT-COCl suspension under stirring for 12 h.

Acknowledgments

References

[1] a) M. Ouyang, J.-L. Huang, C. M. Lieber, *Acc. Chem. Res.* **2002**, *35*, 1018. b) R. H. Baughman, A. A. Zakhidov, W. A. de Heer, *Science* **2002**, *297*, 787.

[2] a) J. Zhang, H. I. Kim, X. Sun, C. H. Oh, H. Lee, *Appl. Phys. Lett.* **2006**, *88*, 053123. b) L. Dai, A. Patil, X. Gong, Z. Guo, L. Liu, Y. Liu, D. Zhu, *ChemPhysChem* **2003**, *4*, 1150. c) O. Zhou, H. Shimoda, B. Gao, S. Oh, L. Fleming, G. Yue, *Acc. Chem. Res.* **2002**, *35*, 1045.

[3] a) S. Banerjee, T. Hemraj-Benny, S. S. Wong, *Adv. Mater.* **2005**, *17*, 17. b) S. Niyogi, M. A. Hamon, H. Hu, B. Zhao, P. Bhowmik, R. Sen, M. E. Itkis, R. C. Haddon, *Acc. Chem. Res.* **2002**, *35*, 1105.

[4] a) S. J. Oh, Y. Cheng, J. Zhang, H. Shimoda, O. Zhou, *Appl. Phys. Lett.* **2003**, *82*, 2521. b) P. Diao, Z. Liu, B. Wu, X. Nan, J. Zhang, Z. Wei, *ChemPhysChem* **2002**, *10*, 898.

[5] S. G. Rao, L. Huang, W. Setyawan, S. Hong, *Nature* **2003**, *425*, 36.

[6] a) N. Nakashima, H. Kobae, T. Sagara, H. Murakami, *ChemPhysChem* **2002**, *5*, 456. b) Z. Chen, Y. Yang, Z. Wu, G. Luo, L. Xie, Z. Liu, S. Ma, W. Guo, *J. Phys. Chem. B* **2005**, *109*, 5473.

[7] a) H. Shimoda, S. J. Oh, H. Z. Geng, R. J. Walker, X. B. Zhang, L. E. McNeil, O. Zhou, *Adv. Mater.* **2002**, *14*, 899. b) R. H. M. Chan, C. K. M. Fung, W. J. Li, *Nanotechnology* **2004**, *15*, s672. c) L. A. Nagahara, I. Amlani, J. Lewenstein, R. K. Tsui, *Appl. Phys. Lett.* **2002**, *80*, 3826.

[8] a) S. Fan, M. G. Chapline, N. R. Franklin, T. W. Tombler, A. M. Casssell, H. Dai, *Science* **1999**, *283*, 512. b) J. Li, H. T. Ng, A. Cassell, W. Fan, H. Chen, Q. Ye, J. Koehne, J. Han, M. Meyyappan, *Nano Lett.* **2003**, *3*, 597.

[9] a) B. Gao, G. Z. Yue, Q. Qiu, Y. Cheng, H. Shimoda, L. Fleming, O. Zhou, *Adv. Mater.* **2001**, *13*, 1770. b) Y. Abe, R. Tomuro, M. Sano, *Adv. Mater.* **2005**, *17*, 2192. c) P. V. Kamat, K. G. Thomas, S. Barazzouk, G. Girishkumar, K. Vinodgopal, D. Meisel, *J. Am. Chem. Soc.* **2004**, *126*, 10757.

[10] a) R. H. M. Chan, C. K. M. Fung, W. J. Li, *Nanotechnology* **2004**, *15*, S672. b) L. A. Nagahara, I. Amlani, J. Lewenstein, R. K. Tsui, *Appl. Phys. Lett.* **2002**, *80*, 3826. c) R. Krupke, F. Hennrich, H. v. Lohneysen, M. M. Kappes, *Science* **2003**, *301*, 344.

[11] a) K. S. Suslick, Y. Didenko, M. M. Fang, T. Hyeon, K. J. Kolbeck, W. B. Mcnamara III, M. M. Mdleleni, M. Wong, *Phil. Trans. R. Soc. Lond. A* **1999**, *357*, 335. b) A. Koshio, M. Yudasaka, M. Zhang, S. Iijima, *Nano Lett.* **2001**, *1*, 361.

[12] a) J. Liu et al, *Science* **1998**, *280*, 1253. b) M. A. Hamon, J. Chen, H. Hu, Y. Chen. M. E. Itkis, A. M. Rao, P. C. Eklund, R. C. Haddon, *Adv. Mater.* **1999**, *11*, 834.

[13] a) S. K. Kim, H. Y. Choi, H. J. Lee, H. Lee, *J. Nanosci. Nanotech.* **2006**, *6*, 3614. b) M. A. Poggi, L. A. Bottomley, P. T. Lillehei, *Nano Lett.* **2004**, *4*, 61.

[14] J. H. Cho, Y. D. Park, D. H. Kim, W. K. Kim, H. W. Jang, J. L. Lee, K. Cho, *Appl. Phys. Lett.* **2006**, *88*, 102104.

[15] U. Dettlaff-Weglikowska, V. Skakalova, R. Graupner, S. H. Jhang, B. H. Kim, H. J. Lee, L. Ley, Y. W. Park, S. Berber, D. Tomanek, S. Roth, *J. Am. Chem. Soc.* **2005**, *127*, 5125.

[16] O. O. Van der Biest, L. J. Vandeperre, *Annu. Rev. Mater. Sci.* **1999**, *29*, 327.

[17] H. Yokoi, T. Kinoshita, S. Zhang, *Proc. Natl. Acad. Sci. USA* **2005**, *102*, 8414.

[18] a) N. Anderson, A. Hartschuh, S. Cronin, L. Novotny, *J. Am. Chem. Soc.* **2005**, *127*, 2533. b) X. Zhang, W. Zhang, L. Liu, Z. X. Shen, *Chem. Phys. Lett.* **2003**, *372*, 497. c) A. M. Rao, J. Chen, E. Richter, U. Schlecht, P. C. Eklund, R. C. Haddon, U. D. Venkateswaran, Y. –K. Kwon, D. Tomanek, *Phys. Rev. Lett.* **2001**, *86*, 3895.

[19] F. Patolsky, Y. Weizmann, I. Willner, *Angew. Chem. Int. Ed.* **2004**, *43*, 2113.

[20] S. Ohnishi, M. Murata, M. Hato, *Biophysical J.* **1998**, *74*, 455.

Supplementary Information for

Vertically Aligned Single-Walled Carbon Nanotube Film Formed by Electrodeposition

Sung-Kyoung Kim[a], Haiwon Lee*[a], Hirofumi Tanaka[b], Paul S. Weiss[c]

[a]   Department of Chemistry, Hanyang University, Seoul 133-794, Korea

[b]   Institute of Molecular Science, Okazaki 444-8787, Japan

[c]   Departments of Chemistry and Physics, The Pennsylvania State University, University Park, PA 16802, USA

E-mail: haiwon@hanyang.ac.kr

Fax: (+82) 2-2296-0287

(carbon nanotube, alignment, electrodeposition, nanosphere lithography, sonication)

AFM & SEM images of shortened SWNTs
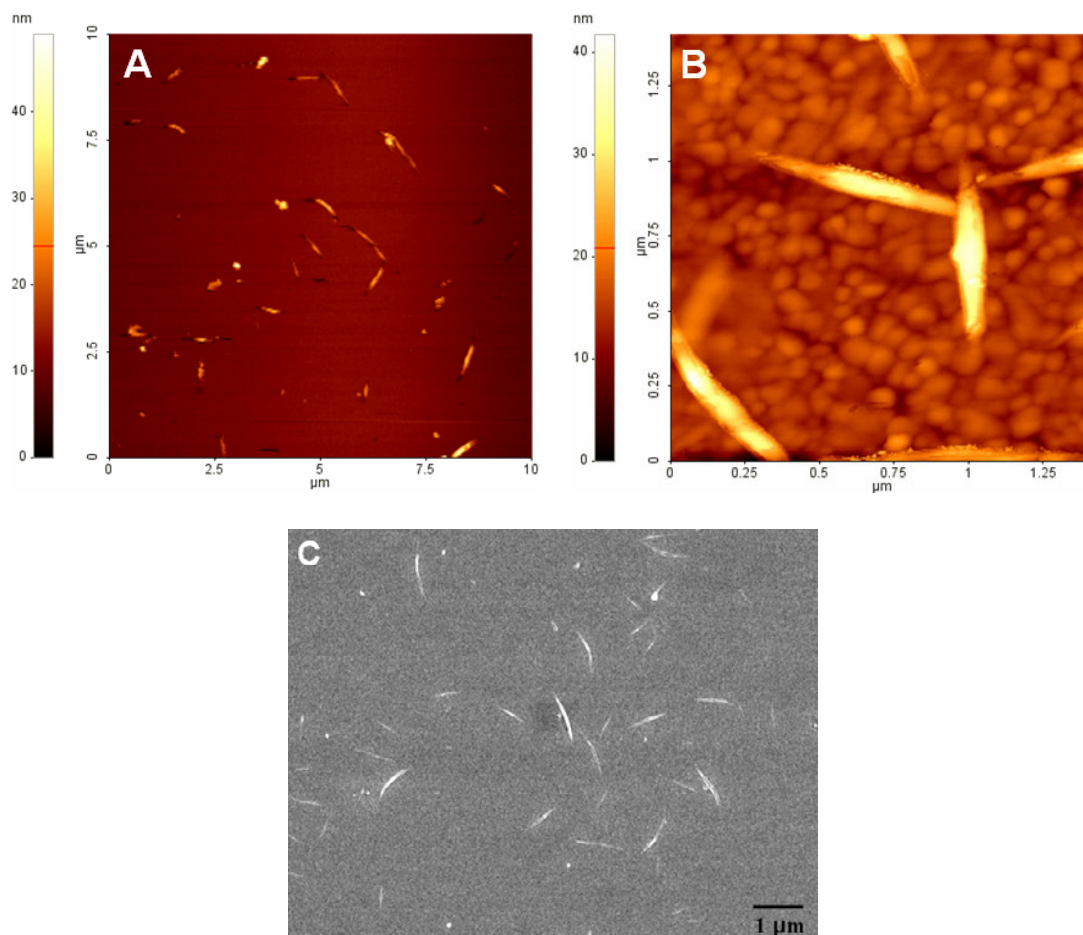
Figure S1. (A) Low resolution & (B) magnified AFM images and (C) SEM image of the shortened SWNTs spread on a substrate.

The shortened and functionalized SWNTs-COCl were spread on a substrate in order to confirm the reduced size of the SWNTs, as shown in Figure S1. From the AFM images, the lengths and diameters of the SWNT bundles after the shortening process were predominantly smaller than 1 µm (typically 600 ± 100 nm) and 50 nm (typically 35 ± 10 nm), respectively.

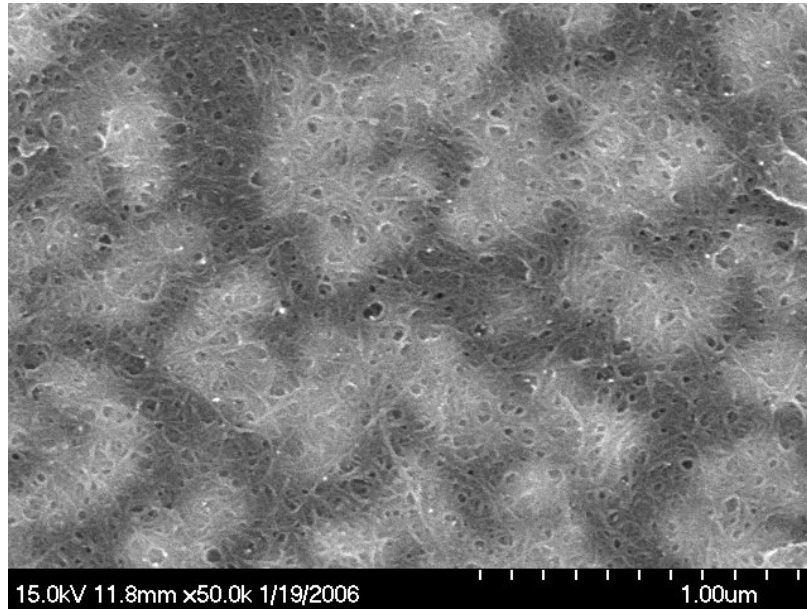**SWNT film electrodeposited in the narrow gap (3.32 mm)**

Figure S2. Scanning electron micrograph of a SWNT film electrodeposited by applying an electric field of 50 V for 10 min to the 3.32 mm gap between the two electrodes.
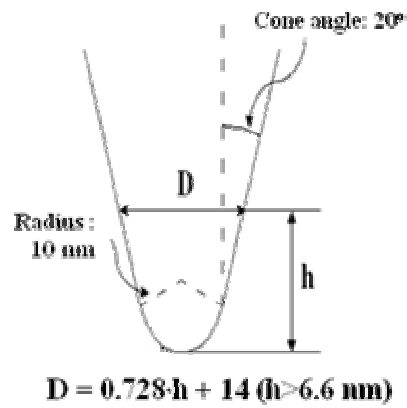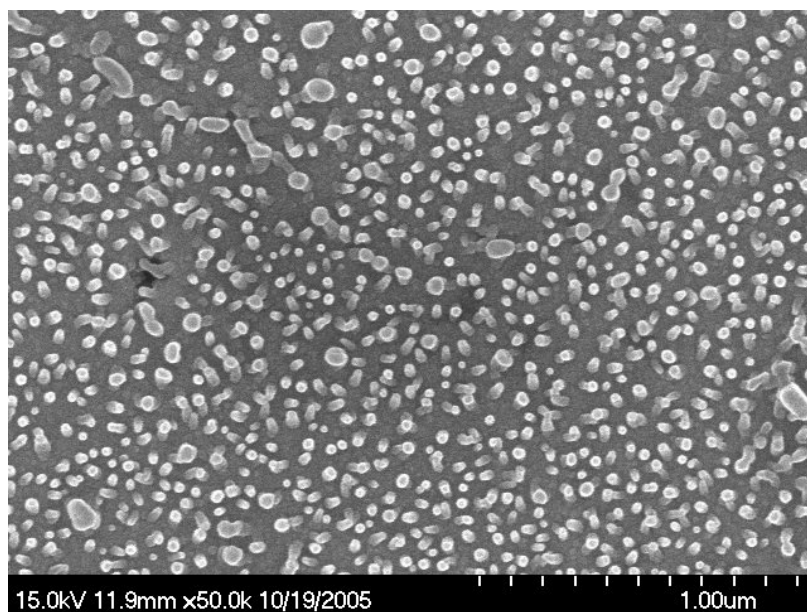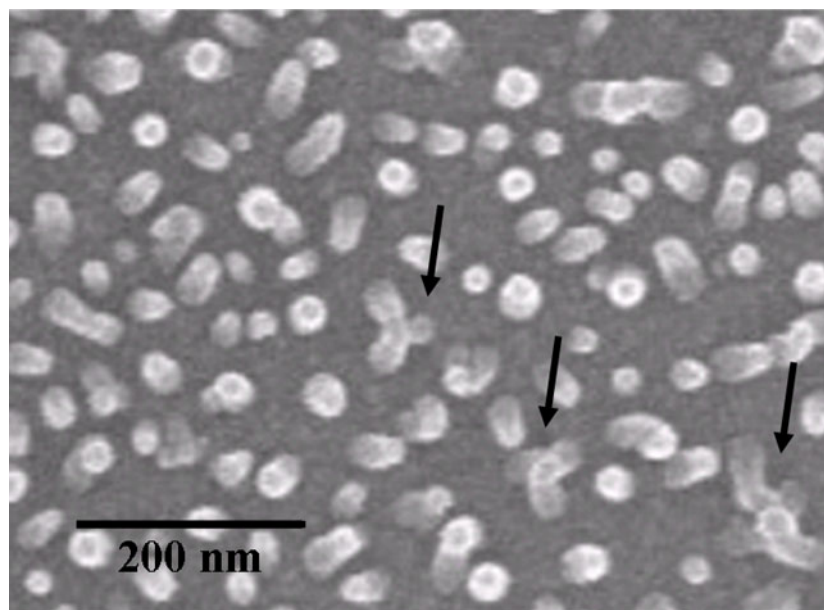
Model tip convolution

$$D = 0.728 \cdot h + 14 \ (h > 6.6 \ nm)$$

Figure S3. Schematic of the conical tip geometry used for imaging SWNT films in tapping mode AFM. The model tip has a cone angle of 20° and a radius of 10 nm. The relation between tip width (**D**) and height (**h**) is expressed as: $D = 0.728 \cdot h + 14$ (h > 6.6 nm).

Magnified image of a vertically aligned SWNT film

(a)

(b)

Figure S4. (a) Scanning electron micrographs of a SWNT film after ultrasonication for 3 min. The film was formed on a gold electrode by applying an electric field at 150 V for 10 min. (b) Magnified image of Figure S4(a). (The arrows indicate the three-bundles-folded structures).

Figure S4 shows details of Figure 2(c). The uniform SWNT film in Figure S4 was electrodeposited on the cathode at a DC voltage of 150 V for 10 min and then ultrasonicated for 3 min. The SWNT bundles were well distributed with uniform space between the bundles and mostly aligned in the direction normal to the surface. The arrows in Figure 4(b) indicate the three-bundles-folded structures that can be observed only in standing structures.

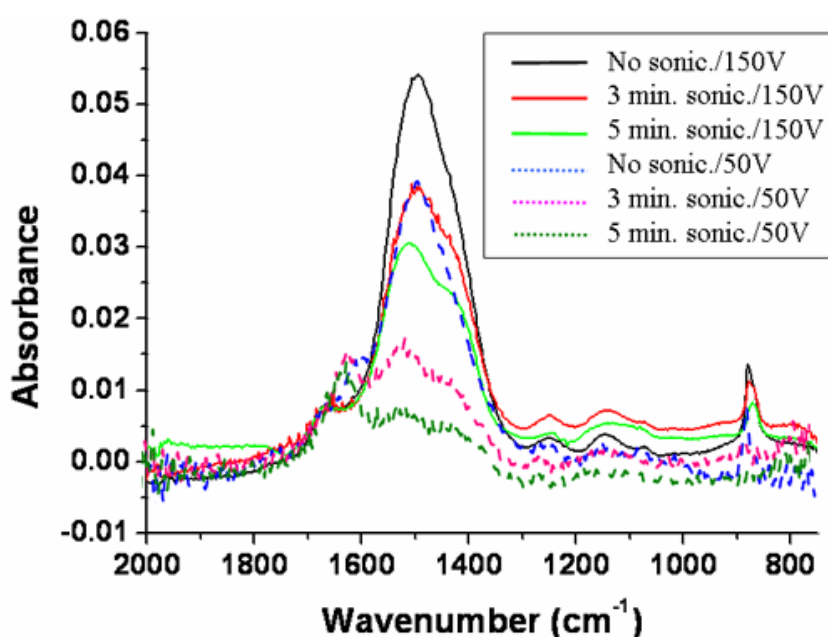**Infrared absorbance of SWNT films**

Figure S5. Variation in infrared absorbance of SWNT films electrodeposited at 150 V and at 50 V with ultrasonication time. The infrared absorbance was obtained from attenuated total reflectance spectra (SENSIR IlluminatIR spectrometer) of the SWNT films. The band at 1500 cm^{-1} corresponds to the stretch mode of the aromatic carbon-carbon bond.